MODEL TESTS WITH A TANKER IN OBLIQUE SEAS

by

E. F. Schulz, T. T. Williams and R. M. Ralston

Civil Engineering Section
Colorado A and M College
Fort Collins, Colorado

Prepared for
David Taylor Model Basin
Navy Department
under Contract N9onr 824(03)
through the
Colorado A and M Research Foundation

January 1957

CER. No. 57EFS2

ABSTRACT

This report presents the results of towing a five-foot model tanker on five different headings in regular long-crested waves of various heights and lengths. The model was free to heave, pitch, and roll. The important parameters affecting the model motions were found to be the effective tuning ratio (ratio of the frequency of encounter to the natural frequency of the model) and the relative wave length (ratio of wave length along the direction of travel to the ship length). The amplitudes of the motions were found to be as much as five times greater than the associated wave function when the tuning ratio was near unity. For a particular tuning ratio the amplitude parameters increased with increasing wave length up to approximately twice the hull length.

CONTENTS

TABLES

FIGURES

Wave Properties

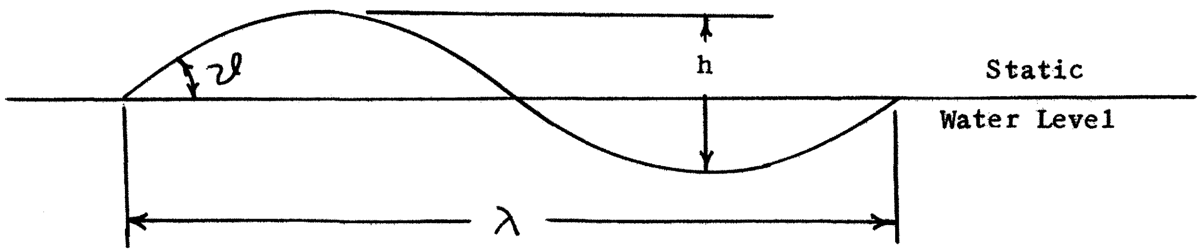

Principal Axes of Ship

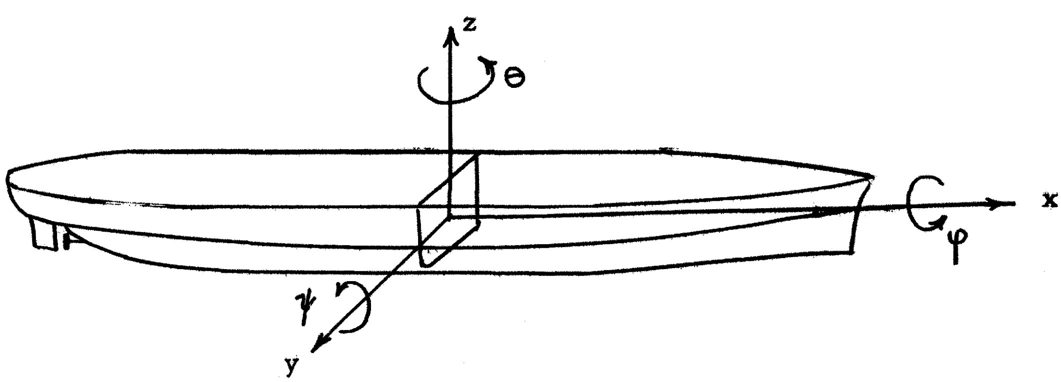

Properties of Seaway

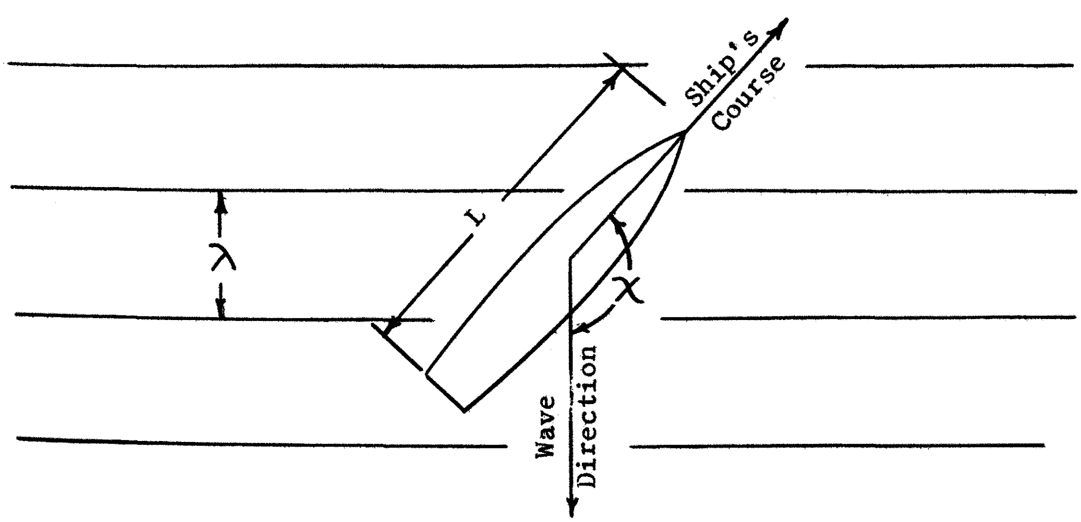

NOTATION

Symbol	Units	Definition
A_m	$(\text{feet})^2$	Area of midship section
A_s	--	Amplitude response factor for s
A_w	$(\text{feet})^2$	Waterplane area
B	feet	Beam
c	feet/sec	Wave celerity
C_B	--	Block coefficient, $\frac{\nabla}{LBD}$
C_M	--	Maximum section coefficient
C_W	--	Waterplane coefficient, $\frac{A_W}{BL}$
D	feet	Draft
Fr	--	Froude number $v \div \sqrt{gL}$
f	cps	Wave frequency
g	ft/sec^2	Acceleration of gravity - $32.16\ ft/sec^2$
h	feet	Wave height (double amplitude)
k	feet	Radius of gyration in xz-plane
L	feet	Waterline length
L_{BP}	feet	Length between perpendiculars
s	--	General motion - maybe, x, y or z or angular, φ, ψ or θ
T_e	seconds	Period of encounter
T_n	seconds	Natural period

Symbol	Units	Definition
v	feet/sec	Speed of model
χ	degrees	Angle of heading of ship relative to direction of wave travel
z	feet	Heave (double amplitude)
α	--	Velocity of ship relative to wave celerity
Λ	--	Tuning ratio
Λ_e	--	Effective tuning ratio
λ	feet	Wave length
ϑ	degrees	Wave slope
ν	radians/sec	Natural frequency
ω	radians/sec	Wave circular frequency
ω_e	radians/sec	Frequency of encounter
ψ	degrees	Angle of pitch
φ	degrees	Angle of roll
Δ	pounds	Displacement of model
∇	$(\text{feet})^3$	Volume of displacement

I. INTRODUCTION

The research work described in this report was conducted for the David Taylor Model Basin, Navy Department, under Contract No. N9onr 824(03). The experiments were carried out in the outdoor 40-ft x 62-ft wave basin previously described in (1).

Approximately 185 test runs were conducted with a model tanker hull during the period June to August 1954. The model was towed at five different headings relative to the direction of travel of a simple wave front.

Through experiments of this type a more complete understanding of seaworthiness can be developed. Seaworthiness is defined as the ability of a ship to remain operational in heavy seas. Designing for seaworthiness is now in a rather uncertain state. Available conclusions are drawn from designs which are known to be particularly good or very bad and some data which have been obtained from towing tests of models heading either into or traveling with the waves. By sailing at some angle other than 0° or 180° relative to the direction of wave travel, one has an opportunity to observe the effects of coupling on the model motions.

The problem of ship motions has also been approached from the theoretical point of view. Some of these studies are reported in (2), (3) and (8). These works are summarized in (4). The equations of motion for coupled pitch and heave have been derived in (8).

II. METHOD AND PROCEDURE

The model used was a 5-ft tanker constructed from fiberglass-plastic laminate and reinforced with aluminum frames. The model characteristics are given in Table 1. The hull lines, wave profile corresponding to a speed of 16 knots, and the sectional area and load waterline are shown in Fig. 1.

Model Loading

Lead ballast was added to the model until the gross weight (41.6 lbs) was equivalent to the design displacement (32,800 tons) scaled down in accordance with the scale factor. The mass was distributed so that the model had the proper radius of gyration in the zx-plane and so that the list and trim were proper relative to the design waterline. The radius of gyration was determined by suspending the loaded model as a torsional pendulum in air from a 20-ft length of steel wire which had been calibrated previously. The list and trim, and the rolling period were determined by observing the appropriate motion while the model was floating in calm water. The radius of gyration thus determined was also checked by swinging the model from a transverse knife edge near the stern. The values of the natural periods are listed in Table 2.

Variables

A list of the variables considered is given in Table 3. Model headings of 0°, 45°, 90°, 135° and 180° were used. On the 0° heading additional tests were conducted for wave lengths of 3.8 ft and 4.6 ft for a height-length ratio of 1:15. The variables listed in Table 3 were reproduced for each of the headings.

III. DESCRIPTION OF EQUIPMENT

The equipment has been previously described in detail in (1). Only new apparatus and modifications will be described here.

Carriage

The suspension bridge consisted of three parallel 1/8-in. diameter high-strength steel wires arranged so as to provide lateral as well as vertical support for the carriage. The wires were supported by the frames of the towing mechanism and idler pulley assembly and approximately 1300 lbs tension was applied to each wire through turnbuckles fastened to buried concrete anchors. Concrete anchors placed at predetermined positions around the pond made it possible to move the bridge to different headings.

Aluminum channel was used for the construction of the carriage in order to keep the weight to a minimum. The carriage was attached to the wires with pulley assemblies which securely clamped the carriage to the bridge. In order to permit free heaving of the model, the carriage engaged a movable vertical stem by means of a roller cage so that only vertical motion was possible. The stem was attached to the model through a gimble ring assembly at the pitching axis. This arrangement permitted the model to roll and pitch freely. Thus the carriage served to propel the model and at the same time to restrain it in the three motions of surge, sway and yaw. Fig. 2 is a photograph of the model attached to the carriage.

Towing was accomplished by means of a $1\frac{1}{2}$ HP induction motor equipped with a magnetic brake. Various speeds were obtained with a step cone pulley assembly combined with a V-belt speed changer. The towing line extended from one side of the carriage to the plastic drive pulley of the towing mechanism, across the pond to an idler pulley assembly, and then back to the other side of the carriage. Constant tension in the towline was maintained by a weight and pulley arrangement on the idler pulley assembly. The towing line was a 1/8 in. diameter nylon cord.

Instrumentation

Instrumentation for measuring the model motions was relatively simple. Heave was measured with a potentiometer mounted on the carriage and actuated by a bow string arrangement on the stem. Since the bridge sagged somewhat from the weight of the carriage, it was necessary to calibrate the heave at regular intervals along the bridge. Pitch and roll were measured with two Y-type convectron tubes mounted at the center of motions of the model. The heave potentiometer and the convectron tubes served as the active elements in typical wheatstone bridge circuits which were coupled to the oscillograph to record the model motions.

The model speed was recorded directly from a $8\frac{1}{4}$ in. diameter plastic idler pulley mounted on the towing mechanism. For each revolution a magnet on the pulley induced a momentary current, in a coil mounted close to the pulley, which was recorded on the oscillograph time scale.

Since movies were also taken on the test runs, synchronization with the oscillograph records was essential. This was accomplished by passing the towline between two closely spaced contacts mounted on the towing mechanism and fastening an aluminum foil sleeve on the towline. The sleeve was placed so that when the model was at the center of the pond, the sleeve closed the contacts, firing a flash bulb mounted on the model and simultaneously producing a mark on the oscillograph record.

Motion Picture Records

Front and side view motion pictures were taken during the tests. These movie records provided a standard for correlating the convectron tube records. These records also yielded information concerning forefoot emergence, bow submergence, stability of the bridge and general suitability of the experiments.

IV. THEORETICAL BACKGROUND

The motion of ships in a seaway is referred to as the seaworthiness. The problem of predicting the seaworthiness of a ship in a real sea is highly complex and consists of two parts. The first is that of predicting how the ship will react to any wave -- even a simple wave. The second part is that of finding a simple mathematical representation for the sea. In order to relate the ship variables to the sea variables in model studies, regular wave trains are substituted for the actual sea.

The model was towed at various headings relative to the direction of travel of a regular wave train. In the analysis each wave was assumed to be of sinusoidal profile and exactly like every other wave. Since the wave is the exciting force causing the motion of the ship, using regular wave trains permits one to express exciting force as a relatively simple mathematical expression. The motion of the ship is the reaction to several forces classified as the inertial forces, the damping forces, and the restoring forces. A general equation of motion is:

$$Q \frac{d^2s}{dt^2} + \ldots N \frac{ds}{dt} + \ldots Rs = F(s,t) \,, \qquad (1)$$

where s is any translational or rotational motion of the ship.

+ ... represents a coupling term,

Q is the inertia coefficient,

N is the damping coefficient,

R is the restoring coefficient.

The analytical problem was simplified by reducing the ship motions under consideration to heave, pitch, and roll. In the case of the model experiments the motions of the ship were restricted to heave, pitch and roll by the restraint applied by the carriage. It has been shown (4) that the heave, pitch or roll at any particular instant can be expressed by the following equations:

$$z = r_m A_z \cos\omega_e t - \epsilon_z - \epsilon'_z \quad , \qquad (2)$$

$$\psi = r_m A_\psi \cos\omega_e t - \epsilon_\psi - \epsilon'_\psi \quad , \qquad (3)$$

$$\varphi = r_m A_\varphi \cos\omega_e t - \epsilon_\varphi - \epsilon'_\varphi \quad , \qquad (4)$$

where r_m is the applicable wave function,

A_s is the amplitude response factor for the particular motion, s

ω_e is the frequency of encounter,

$\epsilon_s + \epsilon'_s$ is the term expressing the total phase shift of the ship's motion relative to the wave.

The wave function, r_m , is the wave slope in the case of the pitch, ψ , and roll, φ . The wave function for heave is the amplitude of the wave or one half the wave height, $\bar{h}$. The frequency of encounter is expressed by:

$$\omega_e = \omega(1 - \alpha) , \qquad (5)$$

where ω is the wave frequency and

α is the relative velocity of the ship in the direction of wave travel, $\alpha = \dfrac{v \cos\chi}{c}$.

V. EXPERIMENTAL RESULTS

Use of Convectron Tubes

The use of Bendix Y-type convectron tubes for measuring angles of pitch and roll was discussed in (1). These devices are somewhat similar to a short period pendulum which can be used in an appropriate electrical circuit to produce easily recorded oscillograph traces of pitching and rolling relative to time. Unfortunately, these convectron tubes are highly sensitive to accelerations. The convectron tube measuring the roll is particularly sensitive to linear accelerations along the y-axis (swaying) and the pitch convectron tube is sensitive to linear accelerations along the x-axis (surging).

The angles of pitch and roll measured by the convectron tubes are compared with the angles as measured from the movie records on Figs. 3 through 7. One run was chosen from each heading for use in this comparison. The magnitude of the acceleration effects on the convectron output is large relative to the output due to the angle of tilt. This makes the convectron tubes difficult to use for ship model studies.

Use of Motion Picture Records

As already mentioned, records of ship motion were made in two different ways: (a) by using an oscillograph to record convectron and potentiometer measurements, and (b) by taking front and side view motion pictures of each run. When the convectron data were found to be unreliable, attention was concentrated on analysis of the ship motions from the motion pictures.

Consideration of several methods of obtaining the necessary measurements from the movie data indicated that the most satisfactory system would be to project the film on a sheet of paper. By stopping the projector at a desired frame, the image of the model, or significant points, could be traced on the paper for later measurements.

Determination of Motions

A flash bulb, mounted on the model, was fired when the model reached the center of the run. The image of the flash was used as a time reference in synchronizing the front and side view films with the oscillograph records. In analyzing each run, the movie film was advanced to the point where the flash occurred (point of synchronization). The film was then advanced one frame at a time until a maximum amplitude of the motion being measured was noted. The position of the model at this maximum was then indicated on the paper. This yielded s_{max} when $ds/dt = 0$. The film was then turned in reverse past the flash to obtain the similar maximum value at the opposite end of the cycle. The total change in the motion then was:

$$\Delta s = s_1 - s_2$$

The side view pictures were used to measure pitch. Two targets were mounted four feet apart on the deck of the model, one near the bow and one near the stern. A horizontal line through the center of the targets was parallel to the design water line. When the frame showing the maximum pitch angle was projected, small crosses were traced from the target images onto the paper. A wire had been stretched horizontally across the wave basin, parallel to the lines of travel of the model, and was easily identified on the projected film by small tags which had been fastened to it at 3-ft intervals. Tracing the image of this wire onto the paper gave a reference line corresponding to a zero pitch angle. To complete reduction of the data, straight lines were drawn on the paper connecting the two sets of crosses, and the angles thus formed with the horizontal datum line were measured with a protractor.

Maximum roll was determined by analyzing the front view film in a manner similar to that described for pitch. Targets had been mounted at either end of a 4-ft aluminum strip fastened horizontally across the deck of the model at the 2.1-ft station. These targets formed the reference points from which to measure maximum values of roll. The rolling period of the model had been adjusted for the inertia effects of this target boom by shifting the ballast. The top of the projected frame was traced onto the paper and used as a datum line from which to measure values of roll to the right or to the left.

Heave was obtained from the side view pictures using the image of the horizontal wire stretched across the basin as a datum. The motion of the reference point on the model relative to the horizontal wire was indicated on the paper.

History of Motion

In order to determine shifts in phase for the various motions it was necessary to produce graphs for each run, showing one or more complete cycles of each motion. This was accomplished by determining the actual value of the motion, pitch, roll or heave, at 1/4-sec time intervals for a period of four seconds. These values were plotted as a function of time. Then by using predetermined envelope values as a guide, it was possible to sketch fairly accurate graphs showing the history of the motion over the four-second period.

To facilitate obtaining the information for these graphs, the film was marked with India ink at 1/4-sec intervals for the period of two seconds preceding and two seconds following the instant when the flash bulb was fired. Since the film had been exposed at a uniform rate of 24 frames per second, this amounted to marking every sixth frame within the given time range.

To obtain the desired values for pitch and roll, the images of the targets and horizontal lines were traced onto the paper for each marked frame. Measurement of the values proceeded in the same manner as for the envelope values.

For heave, the position of the reference point and horizontal wire, and the distance between the targets, was noted on the paper for each marked frame.

As a part of the analysis of the side view pictures a notation was made for each run, indicating the frame closest to the flash at which a wave crest was directly under the pitching axis of the model. The phase shift for each motion then was simply the length of time that maximum motion occurred after this wave passed the midship section of the ship. Knowing the period of encounter, the phase shift could be converted to radians.

Presentation of Data

The primary purpose of this model study was to determine the amplitude parameters when the model was being towed at various headings to a simple wave front. Equations of motion of the ship have been derived from theory. The general equations of motion have been solved for the case of motion induced by regular waves and are shown as Eqs 2, 3 and 4. The amplitude parameter is defined as the ratio of the amplitude of the ship motion to the amplitude of the appropriate wave function. The amplitude parameters were found for a complete cycle of motion using these equations:

For heave,
$$A_z = \frac{\frac{1}{2}\Delta z}{r_m} = \frac{\frac{1}{2}\Delta z}{\frac{1}{2}h} = \frac{\Delta z}{h} \quad , \qquad (5)$$

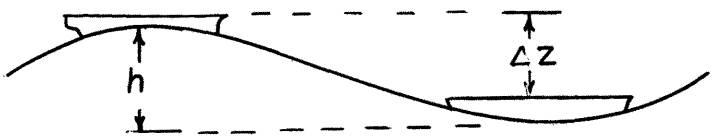

For pitch,
$$A_\psi = \frac{\frac{1}{2}\Delta\psi}{r_m} = \frac{\frac{1}{2}\Delta\psi}{\vartheta} \qquad (6)$$

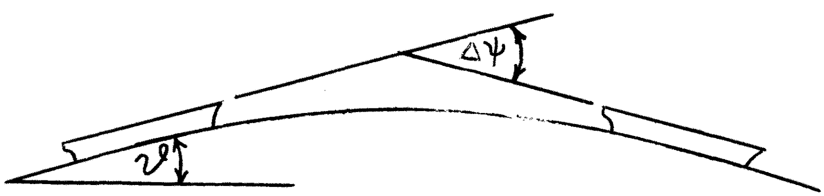

For roll, $$A_\varphi = \frac{\frac{1}{2}\Delta\varphi}{r_m} = \frac{\frac{1}{2}\Delta\varphi}{\vartheta} \quad . \tag{7}$$

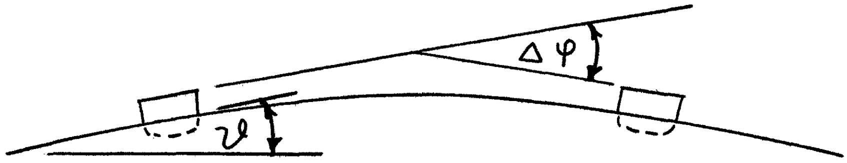

The total phase shift in radians could be obtained from the experimental data from the relationship:

$$\epsilon_s + \epsilon'_s = \omega_e \Delta t \tag{8}$$

where Δt is the time by which the maximum value of the motion lags behind the wave crest.

The effective tuning ratio, $(\Lambda e)_s$, is defined as the ratio of the frequency of encounter to the natural undamped frequency of the vessel.

$$(\Lambda e)_s = \omega_e/\nu_s = \omega/\nu_s \ (1 - \alpha) = \Lambda (1 - \alpha) \ . \tag{9}$$

where ν_s is the natural frequency of the ship in motion, s .

The fundamental measurements taken from the oscillograph and movie records as well as the parameters computed for each test run are shown in Table 4 at the end of this report. Graphs of A_z as a function of $(\Lambda e)_z$, A_ψ as a function of $(\Lambda e)_\psi$ and A_φ as a function of $(\Lambda e)_\varphi$ for each value of λ/L are shown on Figs. 8 through 10.

Forefoot Emergence

An interesting phenomenon observed during some of the model tests was the bow submergence and the forefoot emergence. Wetness of the forward part of the ship is always considered undesirable. Forefoot emergence is associated with slamming. The important factors in slamming are discussed in (7). In addition to forefoot emergence, the phase lag between bow motion and wave motion and the magnitude of relative velocity are considered important factors determining whether or not the ship will slam. Since no accelerometers were used during these experiments, no definite statements can be made concerning slamming. Table 5 has been prepared showing those runs during which bow submergence and forefoot emergence were noted.

VI. DISCUSSION OF RESULTS

Some of the scatter of the data is associated with the heading of the model. The true relative wave length for any particular model and wave combination increases as the heading changes from 0° (or 180°) to 90°. When the ship is sailing at some heading other than 0° and 180°, the ship encounters waves of length $\frac{\lambda}{\cos \chi}$ rather than the nominal wave length, , λ . The mean lines were drawn through the data in accordance with the heading-corrected relative wave length, $\frac{\lambda}{L \cos \chi}$.

λ/L Corrected for Heading

Nominal Relative Wave Length

0°, 180°	45°, 135°	90°
0.72	1.02	∞
0.96	1.36	∞
1.76	2.48	∞

Other reasons for this scatter in amplitude factor are:

1. Variation of the damping due to change of model speed,
2. Variation of the virtual mass caused by interaction of the ship and the waves,
3. "Artificial" coupling introduced by the method of towing or by movement of the towing bridge,
4. Observations of only a few cycles of motion, and
5. Experimental error.

On the 90° heading the frequency of encounter, ω_e, is not influenced by the change of the model speed because the ship has no component of velocity in the direction of wave travel; hence $\alpha = 0$ and $\omega_e = \omega$. For this reason all of the experimental runs at any particular wave length plot on a vertical line on Figs. 8, 9 and 10. The maximum and minimum envelopes for the 90° heading were included in these graphs. In all cases the longest period waves have the highest amplitude parameters. As one might expect, the change as the wave length increases is least important for the pitching motion and most predominate for the rolling motion. The roll amplitude parameters were generally two to four times greater than for pitch or heave. This is attributed to the low damping in roll. Another notable feature of the 90° heading is the reflection of the wave from the seaward side of the ship. The wave is smaller on the leeward side.

Angle of Heading

To gain a clearer picture of the effect of the angle of heading on the amplitude parameters in heave, roll and pitch, they were plotted as a polar diagram in terms of nominal relative wave length λ/L on Fig. 11. These figures show graphically the headings and relative wave lengths producing the largest amplitude factors. The lines were drawn through the mean values of the data and ignore effects due to the different model speeds.

In the case of heave (Fig. 11b), only on the 90° heading and the longest wave length ($\lambda/L = 1.76$) did the average heave amplitude exceed unity; i.e., the heave amplitude was nearly always less than the wave amplitude. Also notable from Fig. 11b is the fact that for all three wave lengths used the model experienced greater heaving in head seas ($\chi = 180°$) than in following seas ($\chi = 0°$) .

The worst conditions as far as pitching is concerned appeared generally on the 180° and 135° heading. The model experienced pitch amplitudes up to 1.2 times the wave slope on the 180° heading in the longest waves ($\lambda/L = 1.76$) . In the case of the shorter waves, the pitching reached greatest amplitudes on the 135° heading for ($\lambda/L = 0.96$) ($\overline{A\psi}_{max} = 0.55$) and on the 45° heading for $\lambda/L = 0.72$ ($\overline{A\psi}_{max} = 0.41$) . In all cases the pitching was least in the shortest waves ($\lambda/L = 0.72$) . In the case of all the wave lengths the least pitching was observed on the 90° heading.

Examination of Fig. 11c shows that the rolling amplitudes were greatest on the 45° heading. This was true for all wave lengths, Normally the rolling is expected to be greater on the 90° heading; however, examination of the data used in Fig. 10 shows that for the wave lengths used in these investigations the effective tuning ratio is nearer unity (resonance) on the 45° heading than on the 90° heading. Hence the roll amplitude parameters tend to be greater on the 45° heading. By decreasing the wave length from $\lambda/L = 1.76$ to 0.72 the mean roll amplitude parameter is reduced on the 45° heading by 3.7 times. ($\overline{A\varphi}_{max} = 0.52$ for $\lambda/L = 0.72$; $\overline{A\varphi}_{max} = 1.85$ for $\lambda/L = 1.76$) .

On the 90° heading the roll amplitude parameter for the two shorter wave lengths was equal, $\overline{A\varphi}_{max} = 0.23$. On the other hand, roll amplitude parameter for the longest wave length was 1.2 or approximately 5 times greater. Here again this is due to the fact that the tests in the longer wave length were nearer resonance, having a tuning factor of approximately 1.3 as compared to 1.8 and 2.0 for the other two wave lengths.

Speed

Correlations of amplitude parameter as a function of speed for various values of heading and relative wave length are shown on Figs. 12, 13 and 14 inclusive. The data were separated by ship motion and by nominal relative wave length, λ/L .

Examination of the data for heave on Fig. 12 shows no decisive trends. The greatest heave amplitude parameters are experienced on the 90° heading for all three wave lengths. For the 90° heading the heave amplitude parameter shows little tendency to increase as the wave length is increased from $\lambda/L = 0.72$ to 1.76 . This seems logical since on this heading the wave encounters all points along the length of the ship simultaneously. The effective relative wave length is infinity $\left(\frac{\lambda}{L \cos \chi} = \infty\right)$. On the other hand, the heave amplitude factors for all other headings progressively increased as the wave length increased from $\lambda/L = 0.72$ to 1.76 . Otherwise the heave amplitude was independent of speed.

The data for pitch are shown on Fig. 13. In general the pitch amplitude parameter decreases as speed increases for the two shorter wave lengths used. In the longest waves tested there are trends indicating increasing pitch amplitude parameters as the speed increases.

This increase in pitching amplitudes in long waves and at high speed was predicted in the analysis found in (8). The longest pitch amplitude parameters experienced were on the 180° heading in the longest waves ($\lambda/L = 1.76$) at the highest speed tested.

The data for the roll amplitude parameters are plotted on Fig. 14. The model responded differently to each relative wave length. There is no logical reason for the model to roll on either the 0° or 180° heading. Some rolling on these two headings did occur. An explanation of this will be offered later. In all cases the rolling amplitudes on these headings were smaller than on any other heading. In all cases the largest roll amplitude parameters occurred on the 45° heading.

On the shortest wave length used, ($\lambda/L = 0.72$) , the rolling was greater at the zero-speed condition than when the model was moving at $Fr \approx 0.1$. Further increase in speed resulted in increase in rolling on the 45° and 90° headings. On the 135° heading, increasing the speed resulted in a decrease in rolling.

When the wave length was increased to $\lambda/L = 0.96$, the roll amplitude parameters were 20 per cent to 30 per cent higher than for the shortest wave length, throughout the entire speed range. When $0<Fr<0.1$, the roll amplitude is virtually independent of speed. Further increase in speed on the 45° heading results in an increase in the roll amplitude parameter until a peak is reached at $Fr = 0.22$. The rolling then decreases with further increase in speed. The roll amplitude parameter is nearly independent of speed on the 90° and 135°

heading which is not in agreement with the generally accepted fact. On these headings the true roll history seems to be masked by the motion of the bridge.

In the longest waves used ($\lambda/L = 1.76$) the roll amplitude parameters are two to three times greater in all cases than in the $\lambda/L = 0.96$ waves. On the 45° heading the roll amplitude parameter increases with increasing speed. On the 90° heading the roll amplitude is independent of speed. On the 135° heading the highest rolling amplitudes occur at the zero-speed and the rolling decreases with increasing speed, which is as one would expect. In all these roll data, the motion of the model is greatly influenced by the swaying of the bridge.

Forefoot Emergence

Those runs during which the model shipped water over the bow and those during which the forefoot emerged are tabulated in Table 5. The length of the emergent forebody is also listed. The 135° and 180° headings were the only headings on which the waves broke over the bow or the forefoot emerged from the wave. It is interesting to note that in every case except one, forefoot emergence was associated with bow submergence. Evidently bow submergence is a less severe form of this motion for this model. This is logical since the conditions of phasing between the wave and the motion are similar for both bow submergence and forefoot emergence.

Forefoot emergence occurred during only one zero-speed run (run 57) at the short wave length ($\lambda/L = 0.72$) on the 135° heading. Incidentally, this is the only run in which bow submergence and forefoot emergence were not associated. This is probably due to the zero-speed condition. In general the forefoot emerged during the lower speed runs ($0 < V < 1.3$ fps) in the short waves ($\lambda/L = 0.72$) ; in the intermediate speed runs ($1.4 < V < 2.0$ fps) in the intermediate waves ($\lambda/L = 0.96$) and during the higher speed runs ($2.4 < V < 3.2$ fps) in the longest waves ($\lambda/L = 1.72$) .

These two undesirable features, forefoot emergence and bow submergence, were observed only on two headings -- 135° and 180°. On the 135° heading 13 cases of bow submergence and six cases of forefoot emergence occurred. Water was taken over the bow during 11 runs and the forefoot emerged during four runs on the 180° heading.

As was pointed out in (7) slamming is not always associated with forefoot emergence; however, forefoot emergence is a necessary requirement for vertical slamming. A second requirement is high relative velocity between ship and wave and the third requirement is the proper phase relationship between bow motion and wave motion. The latter two requirements are related to the tuning ratio. All of the instances where these two phenomena were observed had a tuning ratio in both heave and pitch greater than 0.7. It is interesting to note that while a tuning factor greater than 0.8 is associated with bow submergence, not all runs having a tuning factor greater than 0.8 experienced bow submergence.

Phase Lags

The phase lag between the wave crest at the midship section and the peak amplitude for the three motions were computed. The experimental accuracy in obtaining the time difference from the movie film is poor because of the interactions between the bow wave created by the model, the wave reflections from the side of the ship and the wave itself. These made it difficult to discern the location of the wave crest along the side of the ship. The data have been computed; however, no correlations of the phase shift data are included. Better methods of determining this phase lag in oblique seas must be developed.

<u>Effects of Model Towing</u>

Undoubtedly the manner in which the model was restrained in some of its motions caused the unrestrained motions to be unnatural. Restraint in surging probably affected the heaving, pitching and forefoot emergence. Restraint in swaying probably affected the rolling and heaving. Restraint in yawing probably affected heaving, pitching and rolling.

Because of the relatively long span involved in the suspension bridge, full restraint was not actually realized. Examination of the front view movies indicated that the model swayed considerably. In some cases the carriage traveling on the suspension wires introduced an oscillatory motion similar to that of a system of three bars hinged at four points.

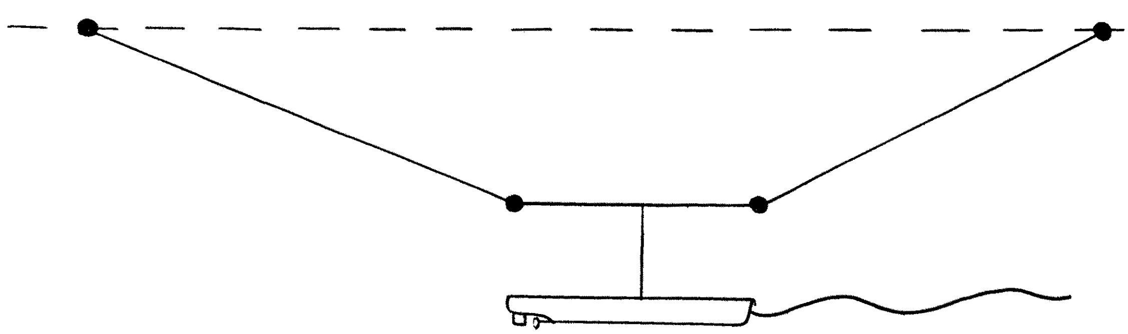

This introduced a complex surging motion.

The heaving was influenced by the natural period of the bridge and carriage in the vertical direction. The natural heaving of the model also tended to relieve periodically some of the load on the suspension wires. Any relief of the load carried by the wires resulted in movement vertically upward and in rotation of the carriage to the left and induced rolling of the model to the right as shown in the following sketch.

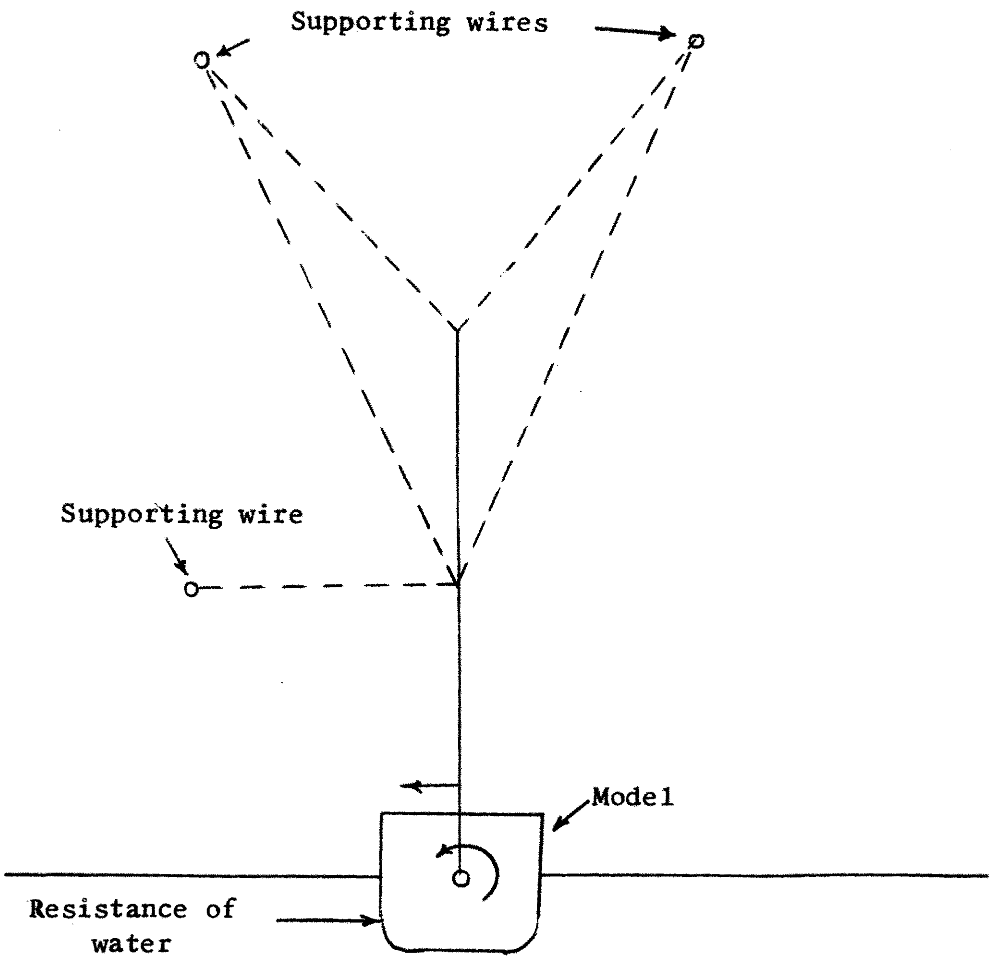

Comparison with Series 60 Model Data

A comparison of the effects of method of towing on the model ship motions was presented in (5). These results for a model of the Todd-Forest Series 60 of the 0.60 block coefficient indicated that this model experienced smaller heaving and pitching amplitudes when the model was restrained in surge compared to a model free to surge. Table 6 shows a comparison of the peak values of pitch and heave amplitude parameters of the Series 60 data from (5) with the tanker data for the $\lambda/L = 0.96$ and $\chi = 180°$ heading. The Series 60 model experienced a 17% reduction of the peak pitch parameter and a 47% reduction of the peak heave parameter when the model was restrained in surge. Comparison of the surge restrained pitch and heave data for the Series 60 model and the tanker shows that the tanker experienced smaller pitch and heave amplitudes. This is as one would expect since the tanker is a full form ship. The hull characteristics of the two hulls are shown in this table.

	Series 60 Model	Model Tanker
Block coefficient, C_B	0.60	0.747
Waterplane coefficient, C_W	0.706	0.821
Entrance angle, $\frac{1}{2}\alpha$	7.0°	27.5°

The results of experiments with a model ship and a rectangular block in regular long crested waves are reported in (6). These data indicate that when $\lambda/L \approx 1.0$, the block experienced smaller pitch and heave parameters than ship form. The pitch and heave parameters were computed from the data published in (6) and are shown in Table 7.

The conclusions from these comparisons are that while the motion of the tanker were approximately one half of the motions for the Series 60 model; these could be expected since the tanker is a full form ship and the tests were restrained in surge.

VII. CONCLUSIONS

Remarks

The heading of the ship directly influences the seaworthiness in two important ways:

1. Causes changes in the frequency of encounter, ωe , and
2. Causes changes in the relative wave length, λ/L .

There may be other effects related to changes of heading due to changes in coupling between the various motions, damping, restoring forces, wave reflection and phase lags.

The amplitude of the motion in heave, pitch or roll is related to the effective tuning ratio, $(\Lambda e)_s$. When the tuning ratio is unity, the frequency of encounter is equal to the natural frequency of the ship and a condition of "resonance" exists. When "resonance" occurs, the response of the ship to the wave is magnified. Peak amplitudes are likely to be as much as three times greater than the associated wave function (see Fig. 10). The magnification is greatest for roll and least for heave.

The peak amplitudes of motion are related to the relative wave length, λ/L or $\frac{\lambda}{L \cos \chi}$. The magnification of the motions is very small for waves shorter than the length of the hull. As the wave length is increased to two times the hull length the amplitude factors increase very rapidly. There is some evidence (Figs. 8 and 9) which indicates that the amplitudes of the motion again decrease after the wave length reaches 2.4 times the hull length.

Increasing the speed has little effect on the heave amplitudes. Here the major factors are heading and relative wave length. Increasing the speed generally causes a decrease in the pitching amplitudes of the ship except in the waves which are longer than the ship and on the 180° heading where increase in speed causes increasing pitching amplitudes.

The model experienced bow submergence and forefoot emergence on the 135° and 180° headings. The forefoot emergence is nearly always associated with bow submergence. The model speed at which these motions occur increases as the wave length increases. These motions were always associated with effective tuning ratios greater than 0.7 in both heave and pitch. Conversely, effective tuning ratios in heave and pitch greater than 0.7 were not always associated with bow submergence and forefoot emergence.

The correlations of the phase shift between the wave crest and peak motions as a function of tuning ratio were very disappointing. These data were taken from the movie records.

Recommendations for Improvements and Future Studies

This project was an exploratory one and the experience gained from this work will prove valuable in future work. A primary requirement of the project was simplicity and minimum expenditure for new facilities.

A bridge consisting of three suspension wires was the best equipment available under the circumstances. Unfortunately, this bridge also responded to the waves through the model and the carriage assembly and it is difficult to determine how the movement of the bridge influenced the natural motions of the model. This bridge has since been replaced by a portable steel truss, supporting rails on which the carriage travels. The new bridge is sufficiently rigid and stable so that it furnishes a fixed datum for measurement.

The cost and effort spent in analyzing the data usually exceeds the cost of conducting the tests. Money spent to reduce analysis time and costs can be advantageous not only to over-all economy but also to the quality of the final data. To this end it is considered essential that all of the equipment and instrumentation should be designed to place all of the desired data on the oscillograph record. An example of this is the frequency of encounter or period of encounter. The period of encounter can be obtained visually from the oscillograph record if a transducer measuring the wave profile is carried by the model or by the carriage. If this transducer is at the midship section, the phase lags can be easily determined.

The model tests should have been extended to somewhat longer waves ($\lambda/L \approx 2.0$) in order to completely verify the tentative conclusion that the amplitude parameters generally peak at this value. The wave length is effectively lengthened by sailing on some heading other than 0° and 180°; however, the coupling is also believed to vary with heading, and if the heading is relied upon to obtain the longer wave lengths, the effects of coupling and relative wave length become inseparable.

The effects of restraining some of the motions on the remaining degrees of freedom should be investigated. It is believed that this same model should be tested as a free self-propelled model to determine the effects of restraints on the motions. While it is true that the effects of steering probably cannot be simulated with a five-foot model, some information can be gained which will assist in making predictions from other model studies.

The effects of extreme changes in ship forms should be investigated by testing other models. The effect of the various hull coefficients on the amplitude parameters and phase lags should be systematically investigated.

REFERENCES

1. Schulz, E. F. Development of a facility for testing the performance of ship hulls in oblique seas. Fort Collins, Colorado A and M College, Civil Engineering Dept. Report No. 54EFS10. March 1954.

2. St. Denis, M. On sustained sea speed. Proc. Soc. Naval Architects and Marine Engineers, New York. Nov. 1951.

3. St. Denis, M. and Pierson, W. J. On the motions of ships in confused seas. Proc. Soc. of Naval Architects and Marine Engineers, New York. Nov. 1953.

4. St. Denis, M. and Pierson, W. J. On some recent developments in the theory of ship motions. Proc. First Conference on Ships and Waves, Richmond, Calif. Oct. 1954.

5. Sibul, O. J. The effect of method of towing on ship motions. Proc. American Towing Tank Conference, Washington, D. C. Sept. 1956.

6. Sibul, O. J. Laboratory studies of the motion of freely floating bodies in non-uniform and uniform long crested waves. Proc. First Conference on Ships and Waves, Richmond, Calif. Oct. 1954.

7. Szebehely, V. G. and Todd, M. A. Ship slamming in head seas. Washington, Taylor Model Basin. Report 913. Feb. 1955.

8. Weinblum G. and St. Denis, M. On the motions of ships at sea. Proc. Soc. Naval Architects and Marine Engineers, New York. Nov. 1950.

T A B L E S

TABLE 1

HULL CHARACTERISTICS OF MODEL TANKER

		Model	Prototype
L_{WL}	Length on waterline, ft	5	600
B	Maximum beam at waterline, ft	0.69	83.51
H	Draft at even keel, ft	0.27	30.64
Δ	Displacement of hull	46.216 lb	32,800 tons
	Scale factor of ship to model length	120	
$\frac{1}{2}$-α	Entrance angle on waterline	27.5°	
C_B	Block coefficient	0.746	
C_M	Maximum (midship) section coefficient	0.993	
C_P	Prismatic coefficient	0.752	
C_W	Waterplane coefficient	0.821	
k	Gyradius in the xz-plane, ft	1.365	165

TABLE 2

NATURAL PERIOD OF MODEL IN WATER

Heave	0.69 sec
Pitch	0.81 sec
Roll	1.69 sec

The natural period was the average of a number of determinations.

The longitudinal radius of gyration was determined by suspending the model in the air at its center of gravity as a torsional pendulum. The period of rotation is given by:

$$T = 2 \sqrt{\frac{Mk^2}{K}},$$

where k = radius of gyration,

T = period of rotation,

M = mass of model,

K = a constant for the wire used = 0.0334 determined by measuring the period of a long slender bar whose k was known.

The rolling period in water was determined from the relationship:

$$T = \frac{0.44B}{\sqrt{GM}}$$

where GM = metacentric height = 0.06B.

TABLE 3

LIST OF VARIABLES

λ Wave Length (feet)	h/λ Height-Length Ratio	V Model Speed (fps)	Fr Froude Number
3.8	1:20	0	0
		1.3	0.1
		2.5	0.2
		3.2	0.25
3.8	1:30	0	0
		1.3	0.1
		2.5	0.2
		3.2	0.25
3.8	1:40	0	0
		1.3	0.1
		2.5	0.2
		3.2	0.25
4.6	1:20	0	0
		1.3	0.1
		2.5	0.2
		3.2	0.25
4.6	1:30	0	0
		1.3	0.1
		2.5	0.2
		3.2	0.25
4.6	1:40	0	0
		1.3	0.1
		2.5	0.2
		3.2	0.25
8.6	1:30	0	0
		1.3	0.1
		2.5	0.2
		3.2	0.25
8.6	1:40	0	0
		1.3	0.1
		2.5	0.2
		3.2	0.25

TABLE 4

EXPERIMENTAL DATA MODEL TANKER TESTS

$\chi = 135°$

λ (feet)	$\frac{\lambda}{L}$	v (fps)	f (cps)	f_e (cps)	h (feet)	$\frac{h}{\lambda}$	ϑ (deg.)	Δz (feet)	A_z	Λ_z	$\Delta\psi$	A_ψ	Λ_ψ	$\Delta\varphi$	A_φ	Λ_φ
4.72	0.944	1.47	1.041	1.261	0.103	0.0218	3.8	0.0288	0.560	0.873	--	--	1.020	--	--	2.136
4.82	0.964	0	1.031	1.031	0.120	0.0249	4.3	--	--	0.714	1.35°	0.157	0.835	--	--	1.746
4.78	0.956	1.45	1.036	1.250	0.092	0.0192	3.3	0.0610	0.6630	0.865	3.55°	0.538	1.012	1.40°	0.212	2.117
4.78	0.956	2.67	1.036	1.431	0.104	0.0218	3.8	0.0552	0.5310	0.991	3.15°	0.444	1.159	0.20°	0.028	2.422
4.82	0.964	3.80	1.031	1.588	0.090	0.0187	3.2	0.0678	0.7534	1.099	2.30°	0.354	1.284	0.80°	0.123	2.686
4.78	0.956	0	1.036	1.036	0.173	0.0362	6.3	0.0599	0.3462	0.717	7.55°	0.604	0.838	1.70°	0.136	1.753
4.72	0.944	1.47	1.041	1.261	0.165	0.0350	6.1	0.1092	0.6618	0.873	8.10°	0.669	1.021	3.00°	0.248	2.138
4.82	0.964	2.02	1.031	1.327	0.181	0.0376	6.5	--	--	0.917	--	--	1.073	6.40°	0.492	2.245
4.82	0.964	2.85	1.031	1.449	0.165	0.0342	5.9	0.0748	0.4534	1.002	6.15°	0.517	1.172	2.50°	0.210	2.450
4.82	0.964	3.83	1.031	1.592	0.168	0.0349	6.0	0.1170	0.6964	1.101	4.80°	0.397	1.289	0.30°	0.023	2.696
4.62	0.924	1.16	1.052	1.229	0.164	0.0355	6.1	0.0967	0.5896	0.850	7.05°	0.530	0.995	--	--	--
4.68	0.936	2.20	1.046	1.378	0.163	0.0348	6.0	0.1144	0.7018	0.954	6.35°	0.525	1.115	1.30°	0.107	2.333
8.79	1.758	0	0.763	0.763	0.243	0.0276	4.8	0.1333	0.5486	0.528	9.15°	0.953	0.617	11.60°	1.208	1.289
8.79	1.758	1.25	0.763	0.863	0.244	0.0278	4.8	0.2340	0.9590	0.597	10.60°	1.093	0.698	--	--	1.459
8.79	1.758	2.45	0.763	0.960	0.245	0.0279	4.8	0.2270	0.9266	0.664	10.25°	1.057	0.777	9.50°	0.979	1.623
8.79	1.758	3.26	0.763	1.025	0.254	0.0289	5.0	0.235	0.9252	0.865	9.65°	0.965	0.831	4.10°	0.410	1.735
8.65	1.730	0	0.770	0.770	0.215	0.0249	4.3	0.189	0.7132	0.533	8.75°	0.994	0.623	10.50°	1.193	1.301
8.92	1.784	1.26	0.758	0.858	0.208	0.0233	4.0	0.183	0.8798	0.594	7.30°	0.912	0.694	3.70°	0.463	1.451
8.79	1.758	1.80	0.763	0.908	0.205	0.0233	4.0	0.192	0.9366	0.628	7.60°	0.950	0.735	5.00°	0.625	1.534
8.92	1.784	3.26	0.758	1.016	0.232	0.0260	4.5	0.243	1.0474	0.703	8.15°	0.906	0.822	4.80°	0.533	1.720
4.77	0.954	0	1.037	1.037	0.236	0.0495	8.6	0.0555	0.2352	0.718	10.05°	0.581	0.840	5.10°	0.295	1.752
4.77	0.954	3.24	1.037	1.516	0.223	0.0468	8.1	0.136	0.6098	1.049	6.50°	0.399	1.227	0.70°	0.043	2.563
4.82	0.964	0	1.031	1.031	0.230	0.0477	8.3	0.121	0.5260	0.714	8.90°	0.571	0.835	5.70°	0.365	1.746
8.83	1.766	0	0.761	0.761	0.242	0.0274	4.7	0.188	0.7768	0.527	9.95°	1.058	0.616	9.10°	0.968	1.287
8.83	1.766	0	0.761	0.761	0.242	0.0274	4.7	--	--	0.527	--	--	0.616	--	--	1.287
3.83	0.766	0	1.157	1.157	0.223	0.0582	10.1	0.088	0.3946	0.800	8.85°	0.438	0.936	6.10°	0.303	1.958
3.92	0.784	1.26	1.142	1.369	0.224	0.0571	9.9	0.0873	0.3898	0.947	7.20°	0.362	1.108	2.00°	0.101	2.319
3.92	0.784	2.50	1.142	--	0.223	0.0569	9.8	0.0808	0.3624	--	4.50°	0.227	--	0.70°	0.036	--
3.83	0.766	2.46	1.157	1.611	0.225	0.0587	10.2	--	--	1.115	--	--	1.303	--	--	2.725
3.79	0.758	3.28	1.162	1.774	0.225	0.0594	10.3	0.046	0.2044	1.228	2.90°	0.141	1.436	1.00°	0.049	3.000
3.88	0.776	0	1.150	1.150	0.144	0.0371	6.4	0.052	0.3612	0.796	5.00°	0.391	0.932	2.10°	0.164	1.948

λ (feet)	$\frac{\lambda}{L}$	v (fps)	f (cps)	f_e (cps)	h (feet)	$\frac{h}{\lambda}$	ϑ (deg.)	Δz (feet)	A_z	Λ_z	$\Delta\psi$	A_ψ	Λ_ψ	$\Delta\varphi$	A_φ	Λ_φ
3.79	0.758	1.29	1.162	1.403	0.143	0.0377	6	0.101	0.7062	0.971	3.90°	0.300	1.135	1.70°	0.131	2.375
3.88	0.776	2.46	1.150	1.598	0.148	0.0381	6.6	0.0392	0.2648	1.106	2.50°	0.189	1.292	0.90°	0.068	2.702
3.96	0.792	3.29	1.137	1.724	0.139	0.0351	6.1	0.0294	0.2116	1.193	2.10°	0.172	1.395	0.50°	0.041	2.819
3.88	0.776	0	1.150	1.150	0.095	0.0245	4.2	0.0359	0.3778	0.796	3.70°	0.441	0.932	1.00°	0.119	1.948
3.84	0.768	1.27	1.154	1.388	0.092	0.0240	4.2	0.0616	0.6696	0.959	2.20°	0.262	1.123	0.80°	0.096	2.350
3.96	0.792	2.44	1.137	1.572	0.090	0.0227	3.9	0.0294	0.3266	1.088	1.50°	0.193	1.272	1.80°	0.231	2.661
3.79	0.758	3.31	1.162	1.779	0.096	0.0253	4.4	0.0358	0.3730	1.230	1.50°	0.171	1.439	0.10°	0.011	3.010

$\chi = 45°$

λ (feet)	$\frac{\lambda}{L}$	v (fps)	f (cps)	f_e (cps)	h (feet)	$\frac{h}{\lambda}$	ϑ (deg.)	Δz (feet)	A_z	Λ_z	$\Delta\psi$	A_ψ	Λ_ψ	$\Delta\varphi$	A_φ	Λ_φ
4.62	0.924	0	1.051	1.051	0.131	0.0284	4.9	0.056	0.4274	0.728	5.75°	0.586	0.851	3.70°	0.378	1.780
4.82	0.964	1.27	1.031	0.840	0.120	0.0249	4.3	0.036	0.3000	0.582	3.05°	0.355	0.680	4.00°	0.466	1.420
4.68	0.936	2.50	1.046	0.668	0.127	0.0271	4.7	0.033	0.2598	0.463	4.20°	0.448	0.541	10.00°	1.065	1.130
4.67	0.934	3.20	1.047	0.562	0.129	0.0276	4.8	0.036	0.2790	0.389	2.60°	0.272	0.454	7.40°	0.770	0.950
4.62	0.924	0	1.051	1.051	0.173	0.0374	6.5	0.055	0.3180	0.728	7.90°	0.607	0.851	6.80°	0.522	1.780
4.72	0.944	1.30	1.041	0.846	0.166	0.0352	6.1	0.0162	0.0976	0.586	5.05°	0.414	0.685	4.75°	0.390	1.430
4.67	0.934	2.50	1.047	0.668	0.170	0.0364	6.3	0.0556	0.3270	0.463	3.75°	0.297	0.541	9.65°	0.765	1.130
4.62	0.924	3.20	1.051	0.561	0.174	0.0377	6.5	0.0283	0.1626	0.388	4.20°	0.323	0.454	6.70°	0.515	0.949
4.82	0.964	3.20	1.031	0.561	0.177	0.0367	6.4	--	--	0.388	--	--	0.454	--	--	0.949
4.67	0.934	0	1.047	1.047	0.209	0.0448	7.8	0.153	0.7320	0.725	9.80°	0.627	0.847	11.75°	0.752	1.770
4.52	0.904	1.30	1.062	0.859	0.225	0.0498	8.6	0.071	0.3156	0.584	6.90°	0.401	0.696	11.80°	0.686	1.452
4.92	0.984	2.50	1.021	0.661	0.218	0.0443	7.7	0.084	0.3852	0.457	5.75°	0.373	0.535	11.25°	0.731	1.118
4.72	0.944	3.20	1.041	0.561	0.225	0.0477	8.3	0.103	0.4578	0.388	5.05°	0.305	0.454	10.45°	0.629	0.949
4.72	0.944	0	1.041	1.041	0.223	0.0472	8.2	0.096	0.4304	0.720	11.15°	0.680	0.843	6.70°	0.409	1.762
4.72	0.944	1.30	1.041	0.846	0.217	0.0460	8.0	0.0357	0.1646	0.586	--	--	0.685	11.65°	0.728	1.430
8.86	1.772	0	0.761	0.761	0.217	0.0245	4.2	0.181	0.8342	0.527	--	--	0.616	6.00°	0.714	1.287
8.86	1.772	1.25	0.761	0.751	0.210	0.0237	4.1	0.154	0.7334	0.519	5.90°	0.720	0.608	18.20°	2.22	1.270
8.96	1.792	2.50	0.755	0.558	0.212	0.0237	4.1	0.1705	0.8042	0.386	6.35°	0.775	0.452	20.70°	2.52	0.945
9.20	1.840	2.44	0.746	0.558	0.208	0.0226	3.9	0.179	0.8606	0.386	6.30°	0.807	0.452	16.45°	2.11	0.945
9.20	1.840	3.20	0.746	0.500	0.212	0.0230	4.0	0.169	0.7972	0.346	5.75°	0.719	0.405	26.30°	3.28	0.846
9.11	1.822	3.22	0.749	0.499	0.212	0.0233	4.0	0.1735	0.8184	0.345	6.00°	0.750	0.404	14.75°	1.84	0.845
9.20	1.840	0	0.746	0.746	0.238	0.0259	4.5	0.225	0.9452	0.516	--	--	0.604	14.60°	1.62	1.261
8.81	1.762	1.25	0.761	0.661	0.243	0.0276	4.8	0.203	0.8354	0.457	7.20°	0.750	0.535	16.17°	1.68	1.118
9.20	1.840	2.44	0.746	0.558	0.238	0.0259	4.5	0.199	0.8362	0.386	6.80°	0.755	0.452	15.83°	1.76	0.945
9.06	1.812	3.21	0.752	0.601	0.250	0.0276	4.8	0.187	0.7480	0.416	6.70°	0.698	0.487	23.92°	2.49	1.016
3.79	0.758	0	1.162	1.162	0.077	0.0203	3.5	0.0325	0.4220	0.805	0.80°	0.114	0.941	4.15°	0.593	1.968
3.88	0.776	1.25	1.150	0.922	0.100	0.0258	4.5	0.0228	0.2280	0.6375	1.15°	0.128	0.746	1.45°	0.161	1.559
3.96	0.792	2.44	1.137	0.701	0.104	0.0263	4.6	0.036	0.3462	0.485	2.00°	0.217	0.567	5.35°	0.581	1.186
3.88	0.776	3.26	1.150	0.556	0.1095	0.0284	4.9	0.0162	0.1480	0.385	1.60°	0.163	0.450	3.70°	0.378	0.940
3.89	0.778	0	1.148	1.148	0.133	0.0342	5.9	0.0226	0.1700	0.794	4.75°	0.402	0.930	1.65°	0.140	1.941
3.83	0.766	1.25	1.157	0.926	0.136	0.0355	6.1	0.0292	0.2148	0.640	3.65°	0.299	0.750	2.80°	0.230	1.567

TABLE 4 --Continued

λ (feet)	$\frac{\lambda}{L}$	v (fps)	f (cps)	f_e (cps)	h (feet)	$\frac{h}{\lambda}$	ϑ (deg.)	Δz (feet)	A_z	Λz	$\Delta\psi$	A_ψ	$\Lambda\psi$	$\Delta\varphi$	A_φ	$\Lambda\varphi$
3.88	0.776	2.20	1.150	0.705	0.135	0.0348	6.0	0.0258	0.1912	0.4875	3.15°	0.262	0.571	6.60°	0.550	1.192
3.88	0.776	3.26	1.150	0.556	0.133	0.0343	5.9	0.067	0.3200	0.385	2.35°	0.199	0.450	8.15°	0.690	0.940
3.88	0.776	2.44	1.150	0.705	0.139	0.0358	6.2	0.0226	0.1626	0.4875	3.20°	0.258	0.571	6.15°	0.497	1.192
				$\chi = 90°$												
3.79	0.758	0	1.163	1.163	0.220	0.0580	10.0	0.225	1.022	0.805	2.60°	0.130	0.942	5.55	0.277	1.968
3.79	0.758	1.24	1.163	1.163	0.215	0.0567	9.8	0.234	1.088	0.805	1.90°	0.097	0.942	3.20°	0.163	1.968
3.79	0.758	2.42	1.163	1.163	0.225	0.0594	10.3	0.226	1.004	0.805	3.50°	0.170	0.942	2.25°	0.109	1.968
3.88	0.776	3.24	1.150	1.150	0.207	0.0534	9.2	0.212	1.024	0.796	3.35°	0.182	0.932	3.30°	0.179	1.947
3.88	0.776	0	1.150	1.150	0.108	0.0278	4.8	0.1075	0.996	0.796	2.15°	0.224	0.932	3.85°	0.401	1.947
3.88	0.776	1.25	1.150	1.150	0.127	0.0327	5.7	0.115	0.906	0.796	0.80°	0.070	0.932	0.50°	0.044	1.947
3.88	0.776	2.44	1.150	1.150	0.126	0.0325	5.6	0.144	1.142	0.796	1.95°	0.174	0.932	2.10°	0.188	1.947
3.88	0.776	3.24	1.150	1.150	0.130	0.0335	5.8	0.146	1.124	0.796	1.80°	0.155	0.932	2.55°	0.220	1.947
3.75	0.750	0	1.168	1.168	0.114	0.0304	5.3	0.065	0.570	0.808	0.50°	0.048	0.946	0.70°	0.066	1.979
3.75	0.750	1.24	1.168	1.168	0.100	0.0267	4.6	0.082	0.820	0.808	0.75°	0.082	0.946	0.25°	0.027	1.979
3.75	0.750	2.44	1.168	1.168	0.103	0.0275	4.8	0.099	0.962	0.808	1.35°	0.141	0.946	1.80°	0.187	1.979
3.75	0.750	3.26	1.168	1.168	0.096	0.0256	4.4	0.085	0.886	0.808	1.75°	0.198	0.946	2.00°	0.228	1.979
4.62	0.924	0	1.052	1.052	0.150	0.0325	5.6	0.146	0.974	0.728	3.85°	0.344	0.933	1.90°	0.169	1.782
4.62	0.924	1.25	1.052	1.052	0.130	0.0281	4.8	0.139	1.070	0.728	2.00°	0.208	0.933	2.15°	0.224	1.782
4.62	0.924	2.44	1.052	1.052	0.153	0.0331	5.7	0.141	0.922	0.728	--	--	0.933	2.50°	0.219	1.782
4.62	0.924	3.26	1.052	1.052	0.129	0.0279	4.8	0.120	0.930	0.728	1.35°	0.141	0.933	1.75°	0.182	1.782
4.62	0.924	0	1.052	1.052	0.202	0.0437	7.6	0.167	0.826	0.728	1.35°	0.089	0.933	2.80°	0.184	1.782
4.72	0.944	2.42	1.041	1.041	0.190	0.0403	7.0	0.168	0.884	0.721	1.20°	0.085	0.925	1.90°	0.135	1.763
4.62	0.924	3.23	1.052	1.052	0.200	0.0433	7.5	0.153	0.766	0.728	2.60°	0.173	0.933	1.85°	0.123	1.782
4.67	0.934	0	1.047	1.047	0.268	0.0574	9.9	0.277	1.034	0.724	1.55°	0.078	0.928	3.85°	0.194	1.772
4.72	0.944	1.25	1.041	1.041	0.275	0.0583	10.1	0.280	1.018	0.721	1.50°	0.074	0.925	4.75°	0.235	1.763
4.62	0.924	2.44	1.052	1.052	0.265	0.0574	9.9	0.244	0.920	0.728	2.20°	0.111	0.933	2.55°	0.129	1.782
4.72	0.944	3.26	1.041	1.041	0.277	0.0587	10.2	0.269	0.972	0.721	3.55°	0.174	0.925	2.15°	0.105	1.763
8.79	1.758	0	0.764	0.764	0.233	0.0265	4.6	0.293	1.258	0.528	0.65°	0.071	0.619	12.20°	1.275	1.293
8.79	1.758	1.25	0.764	0.764	0.254	0.0289	5.0	0.264	1.040	0.528	1.90°	0.190	0.619	11.40°	1.140	1.293
8.79	1.758	2.44	0.764	0.764	0.257	0.0292	5.1	0.286	1.112	0.528	1.75°	0.171	0.619	13.75°	1.347	1.293
8.79	1.758	3.24	0.764	0.764	0.261	0.0297	5.1	0.290	1.112	0.528	1.45°	0.142	0.619	9.55°	0.936	1.293
8.79	1.758	3.27	0.764	0.764	0.256	0.0291	5.0	0.251	0.980	0.528	0.80°	0.080	0.619	15.80°	1.580	1.293
8.92	1.784	0	0.758	0.758	0.210	0.0235	4.1	0.206	0.980	0.525	0.45°	0.055	0.615	6.55°	1.360	1.283
8.79	1.758	1.25	0.764	0.764	0.220	0.0250	4.3	0.190	0.864	0.528	2.10°	0.244	0.619	11.70°	1.210	1.293
8.79	1.758	2.44	0.764	0.764	0.223	0.0254	4.4	0.232	1.040	0.528	1.00°	0.113	0.619	10.65°	1.315	1.293
8.65	1.730	3.28	0.770	0.770	0.216	0.0250	4.3	0.231	1.070	0.533	1.50°	0.174	0.624	11.30°	--	1 303

λ (feet)	$\frac{\lambda}{L}$	v (fps)	f (cps)	f_e (cps)	h (feet)	$\frac{h}{\lambda}$	ϑ (deg.)	Δz (feet)	A_z	Λ_z	$\Delta\psi$	A_ψ	Λ_ψ	$\Delta\varphi$	A_φ	Λ_φ
				$\chi = 180°$												
8.82	1.764	0	0.761	0.761	0.230	0.0261	4.5	0.151	0.6566	0.527	9.3°	1.032	0.616	1.55°	0.172	1.287
8.82	1.764	1.22	0.761	0.899	0.220	0.0249	4.3	0.178	0.8090	0.622	9.8°	1.140	0.727	2.25°	0.261	1.521
8.82	1.764	2.37	0.761	1.030	0.227	0.0257	4.5	0.215	0.9472	0.713	11.2°	1.245	0.834	1.70°	0.189	1.745
8.82	1.764	3.18	0.761	1.122	0.220	0.0249	4.3	0.216	0.9818	0.777	11.7°	1.360	0.908	2.35°	0.273	1.900
9.06	1.812	3.19	0.752	1.104	0.227	0.0251	4.3	0.222	0.9780	0.754	12.3°	1.425	0.894	1.60°	0.186	1.870
9.06	1.812	3.18	0.752	1.103	0.232	0.0256	4.4	0.241	1.0388	0.753	12.4°	1.410	0.893	--	--	1.869
8.82	1.764	0	0.761	0.761	0.290	0.0329	5.7	0.198	0.6828	0.527	9.7°	0.850	0.616	5.80°	0.509	1.287
8.82	1.764	1.22	0.761	0.899	0.271	0.0307	5.3	0.188	0.6938	0.622	12.2°	1.150	0.727	5.20°	0.491	1.521
8.82	1.764	2.39	0.761	1.032	0.252	0.0286	5.0	0.236	0.9376	0.715	12.8°	1.280	0.836	1.05°	0.105	1.747
8.82	1.764	3.20	0.761	1.124	0.267	0.0303	5.2	0.287	1.0750	0.778	13.0°	1.250	0.910	1.25°	0.121	1.903
4.82	0.964	0	1.031	1.031	0.138	0.0286	5.0	0.0165	0.1196	0.714	3.8°	0.380	0.835	0.00°	0	1.746
4.78	0.956	1.22	1.035	1.290	0.133	0.0278	4.8	0.054	0.4060	0.893	6.3°	0.656	1.044	2.30°	0.239	2.184
4.78	0.956	2.40	1.035	1.537	0.132	0.0276	4.8	0.0484	0.3666	1.061	2.7°	0.286	1.243	0.90°	0.042	2.600
4.74	0.948	3.22	1.040	1.719	0.141	0.0297	5.1	0.0377	0.2674	1.189	1.4°	0.137	1.391	0.35°	0.034	2.809
4.74	0.948	0	1.040	1.040	0.195	0.0411	7.1	0.0168	0.0864	0.720	3.7°	0.261	0.842	2.00°	0.141	1.761
4.74	0.948	1.22	1.040	1.297	0.205	0.0432	7.5	0.063	0.3074	0.896	7.5°	0.500	1.049	2.73°	0.182	2.194
4.74	0.948	2.40	1.040	1.546	0.210	0.0443	7.7	0.0508	0.2420	1.069	3.5°	0.227	1.251	0.00°	0	2.618
4.78	0.956	3.18	1.035	1.700	0.212	0.0444	7.7	0.0500	0.2358	1.177	2.2°	0.143	1.377	0.00°	0	2.878
4.72	0.944	0	1.041	1.041	0.282	0.0597	10.3	0.0241	0.0854	0.721	7.9°	0.379	0.843	1.00°	0.048	1.762
4.62	0.924	1.21	1.051	1.313	0.315	0.0682	11.8	0.0629	0.1996	0.908	10.8°	0.458	1.062	2.35°	0.099	2.223
4.64	0.928	2.40	1.050	1.567	0.295	0.0636	11.0	0.0629	0.2132	1.073	5.6°	0.254	1.268	1.80°	0.082	2.650
4.62	0.924	3.21	1.051	1.746	0.290	0.0628	10.9	0.0318	0.1096	1.208	3.5°	0.161	1.413	0.90°	0.041	2.955
3.58	0.716	0	1.196	1.196	0.275	0.0768	13.3	0.0414	0.1506	0.827	2.9°	0.109	0.967	0.00°	0	2.023
3.54	0.708	1.23	1.203	1.550	0.258	0.0729	12.6	0.0614	0.2380	1.072	0.8°	0.032	1.255	1.60°	0.063	2.623
3.53	0.706	2.40	1.205	1.885	0.265	0.0751	13.0	0.0414	0.1562	1.304	0.5°	0.019	1.526	0.75°	0.024	3.190
3.54	0.708	3.22	1.203	2.113	0.253	0.0715	12.4	0.0366	0.1446	1.461	0.6°	0.024	1.711	0.70°	0.023	3.575
3.54	0.708	0	1.203	1.203	0.188	0.0531	9.2	0.0217	0.1154	0.832	1.5°	0.081	0.974	0.00°	0	2.036
3.54	0.708	1.23	1.203	1.550	0.185	0.0523	9.1	0.0218	0.1178	1.072	0.3°	0.016	1.255	0.60°	0.033	2.623
3.54	0.708	2.40	1.203	1.881	0.179	0.0506	8.8	0.0170	0.0950	1.031	0.3°	0.017	1.523	0.00°	0	3.183
3.54	0.708	3.22	1.203	2.113	0.179	0.0506	8.8	0.0264	0.1474	1.461	0.15°	0.008	1.711	0.90°	0.051	3.575
3.58	0.716	0	1.196	1.196	0.137	0.0383	6.6	0.0169	0.1234	0.827	1.8°	0.136	0.967	0.00°	0	2.023
3.58	0.716	1.23	1.196	1.540	0.128	0.0358	6.2	0.0168	0.1312	1.066	0.45°	0.033	1.247	0.35°	0.023	2.606
3.61	0.722	2.41	1.190	1.858	0.123	0.0341	5.9	0.0121	0.0984	1.285	0.15°	0.012	1.504	0.00°	0	3.143
3.61	0.722	3.23	1.190	2.085	0.126	0.0349	6.0	0.0121	0.0960	1.443	0.40°	0.033	1.688	0.00°	0	3.528

TABLE 4 --Continued

λ (feet)	$\frac{\lambda}{L}$	v (fps)	f (cps)	f_e (cps)	h (feet)	$\frac{h}{\lambda}$	ϑ (deg.)	Δz (feet)	A_z	Λ_z	$\Delta\psi$	A_ψ	Λ_ψ	$\Delta\varphi$	A_φ	Λ_φ
				$\chi = 0°$												
3.44	0.688	0	1.122	1.122	0.285	0.0828	14.3	0.0580	0.2036	0.776	4.80°	0.168	0.909	0.80°	0.028	1.900
3.44	0.688	1.24	1.122	0.762	0.286	0.0831	14.4	0.0242	0.0846	0.527	2.55°	0.088	0.617	0	0	1.289
3.44	0.688	2.42	1.122	0.419	0.294	0.0855	14.8	0.0239	0.0812	0.290	1.60°	0.054	0.339	0.70°	0.024	0.709
3.44	0.688	3.24	1.122	0.280	0.297	0.0863	14.9	0.0215	0.0724	0.194	0.00°	0	0.227	0	0	0.473
3.41	0.682	0	1.225	1.225	0.251	0.0736	12.8	0.0384	0.1530	0.847	3.50°	0.136	0.992	0.70°	0.027	2.072
3.41	0.682	1.24	1.225	0.861	0.230	0.0674	11.7	0.0144	0.0626	0.596	2.00°	0.085	0.697	0.20°	0.008	1.456
3.41	0.682	2.42	1.225	0.515	0.248	0.0727	12.6	0.0289	0.1166	0.366	0.55°	0.022	0.417	0.70°	0.027	0.871
3.41	0.682	2.42	1.225	0.515	0.234	0.0686	11.9	0.0241	0.1030	0.366	0.90°	0.038	0.417	--	--	0.871
3.41	0.682	3.24	1.225	0.275	0.248	0.0727	12.6	0.0219	0.0350	0.190	2.15°	0.085	0.223	0.70°	0.028	0.465
3.41	0.682	0	1.225	1.225	0.146	0.0428	7.4	0.0314	0.2150	0.847	1.95°	0.132	0.992	0	0	2.072
3.41	0.682	1.24	1.225	0.861	0.148	0.0434	7.5	0.0220	0.1486	0.596	0.60	0.040	0.697	0	0	1.456
3.41	0.682	2.43	1.225	0.512	0.158	0.0463	8.0	0.0193	0.1222	0.354	0.70°	0.044	0.414	0	0	0.865
3.41	0.682	3.24	1.225	0.275	0.150	0.0440	7.6	0.0222	0.1480	0.190	1.30°	0.085	0.223	0.10°	0.0066	0.465
4.77	0.954	0	1.045	1.045	0.118	0.0247	4.3	0.0098	0.0826	0.723	4.50°	0.522	0.846	0	0	1.768
4.77	0.954	1.24	1.045	0.875	0.126	0.0264	4.6	0.0193	0.1532	0.543	2.25°	0.245	0.636	0.30°	0.0326	1.328
4.77	0.954	2.43	1.045	0.536	0.123	0.0258	4.5	0.0193	0.1570	0.371	2.00°	0.222	0.434	0	0	0.906
4.64	0.928	3.22	1.050	0.356	0.138	0.0297	5.1	0.0170	0.1232	0.246	0.07°	0.007	0.288	0	0	0.602
4.77	0.954	0	1.045	1.045	0.185	0.0388	6.7	0.0144	0.0778	0.723	5.50°	0.411	0.846	0	0	1.768
4.77	0.954	1.24	1.045	0.785	0.186	0.0390	6.8	0.0217	0.1166	0.543	2.70°	0.198	0.636	0.50°	0.037	1.328
4.77	0.954	2.43	1.045	0.536	0.188	0.0394	6.8	0.0194	0.1032	0.371	3.20°	0.235	0.434	0	0	0.906
4.77	0.954	3.26	1.045	0.362	0.183	0.0384	6.6	0.0250	0.1366	0.250	3.65°	0.276	0.293	0.60°	0.0454	0.612
4.72	0.944	0	1.041	1.041	0.255	0.0540	9.4	0.0314	0.1232	0.721	9.00°	0.479	0.843	1.70°	0.0904	1.762
4.72	0.944	1.25	1.041	0.776	0.260	0.0551	9.5	0.0241	0.0926	0.537	4.65°	0.245	0.628	0.30°	0.0158	1.312
4.72	0.944	2.43	1.041	0.526	0.268	0.0568	9.8	0.0169	0.0630	0.364	2.80°	0.143	0.426	0	0	0.889
4.72	0.944	3.26	1.041	0.350	0.278	0.0589	10.2	0.0291	0.1046	0.242	2.45°	0.120	0.283	0.20°	0.0098	0.592
4.72	0.944	0	1.041	1.041	0.304	0.0644	11.1	0.0121	0.0398	0.721	10.05°	0.453	0.843	3.50°	0.157	1.762
4.72	0.944	1.24	1.041	0.778	0.302	0.0640	11.1	0.0217	0.0718	0.538	5.20°	0.234	0.630	0.70°	0.031	1.318
4.72	0.944	2.42	1.041	0.528	0.327	0.0693	12.0	0.0145	0.0444	0.366	3.75°	0.156	0.428	0.70°	0.029	0.894
4.92	0.984	3.26	1.021	0.358	0.302	0.0614	10.6	0.0291	0.0964	0.248	2.90°	0.136	0.290	2.40°	0.113	0.606
8.79	1.758	0	0.764	0.764	0.217	0.0247	4.3	0.1705	0.7858	0.528	10.00°	1.162	0.618	3.50°	0.407	1.293
8.96	1.792	1.24	0.755	0.617	0.210	0.0234	4.1	0.1873	0.8920	0.427	9.00°	1.097	0.499	1.80°	0.219	1.044
8.83	1.766	2.42	0.760	0.486	0.217	0.0246	4.3	0.1772	0.8166	0.336	7.30°	0.848	0.393	3.55°	0.412	0.821
8.79	1.758	3.24	0.763	0.394	0.220	0.0250	4.3	0.1720	0.7818	0.272	7.45°	0.866	0.319	3.15°	0.366	0.667
8.79	1.758	0	0.763	0.763	0.210	0.0239	4.1	0.1429	0.6804	0.528	8.20°	1.000	0.617	3.75°	0.457	1.289
8.83	1.766	1.25	0.761	0.519	0.198	0.0224	3.9	0.1513	0.7642	0.359	7.10°	0.910	0.420	2.45°	0.314	0.878
8.79	1.758	2.40	0.763	0.490	0.192	0.0218	3.8	0.1586	0.8260	0.339	6.90°	0.908	0.397	3.60°	0.474	0.828
8.79	1.758	3.23	0.763	0.396	0.186	0.0212	3.7	0.1439	0.7736	0.274	7.10°	0.960	0.321	--	--	0.670

TABLE 5

OCCURRENCE OF BOW SUBMERGENCE OR FOREFOOT EMERGENCE

Heading	λ (ft)	h (ft)	h/λ	v (fps)	Length of Forebody Exposed (ft)	Shipped Water Over Bow	Λz	$\Lambda \psi$
135°	4.72	.165	.0350	1.47	0.68	Yes	0.873	1.021
	4.82	.181	.0376	2.02	0.55	"	0.917	1.073
	4.82	.165	.0342	2.85	-	"	1.002	1.172
	4.82	.168	.0349	3.83	-	"	1.101	1.289
	4.62	.164	.0355	1.16	0.25	"	0.850	0.995
	4.68	.163	.0348	2.20	0.49	"	0.954	1.115
	8.79	.254	.0289	3.26	-	"	0.865	0.831
	8.92	.232	.0260	3.26	-	"	0.703	0.822
	4.77	.223	.0468	3.24	-	"	1.049	1.227
	3.83	.223	.0582	0	0.26	No	0.800	0.936
	3.92	.224	.0571	1.26	0.54	Yes	-	-
	3.92	.225	.0569	2.46	-	"	1.115	1.303
	3.79	.225	.0594	3.28	-	"	1.228	1.436
	3.96	.139	.0351	3.29	-	"	1.193	1.395
180°	8.82	.227	.0257	2.37	-	"	0.713	0.834
	8.82	.220	.0249	3.18	-	"	0.777	0.908
	9.06	.227	.0251	3.19	-	"	0.754	0.894
	9.06	.232	.0256	3.18	-	"	0.753	0.893
	8.82	.252	.0286	2.59	0.42	"	0.715	0.836
	8.82	.267	.0303	3.20	0.32	"	0.778	0.910
	4.74	.205	.0432	1.22	0.28	"	0.896	1.049
	4.62	.315	.0682	1.21	0.75	"	0.908	1.062
	4.64	.295	.0636	2.40	-	"	1.073	1.268
	4.62	.290	.0628	3.21	-	"	1.208	1.413
	3.83	.256	.0670	3.20	-	"	1.461	1.711

TABLE 6

COMPARISON OF SERIES 60 MODEL AND MODEL TANKER DATA
$\chi = 180°$ (head seas)

Series 60 Model, Block Coefficient 0.60, $\lambda/L = 1.0$	Max. A_ψ	Max. A_z	Tanker Block Coefficient 0.75, $\lambda/L = 0.96$ Max. A_ψ	Max. A_z
Free to Surge	0.99	1.64	-	-
Surge restrained	0.82	0.87	0.50	0.42

TABLE 7

COMPARISON PITCHING AND HEAVING OF A MODEL SHIP AND A BLOCK
$\chi = 180°$ (head seas)

Model Ship (Clairton) $\lambda/L = 1.09$, $L = 3.9$ ft A_ψ	A_z	Block $\lambda/L = 1.19$, $L = 0.995$ ft A_ψ	A_z
0.59	0.37	0.08	0.11

F I G U R E S

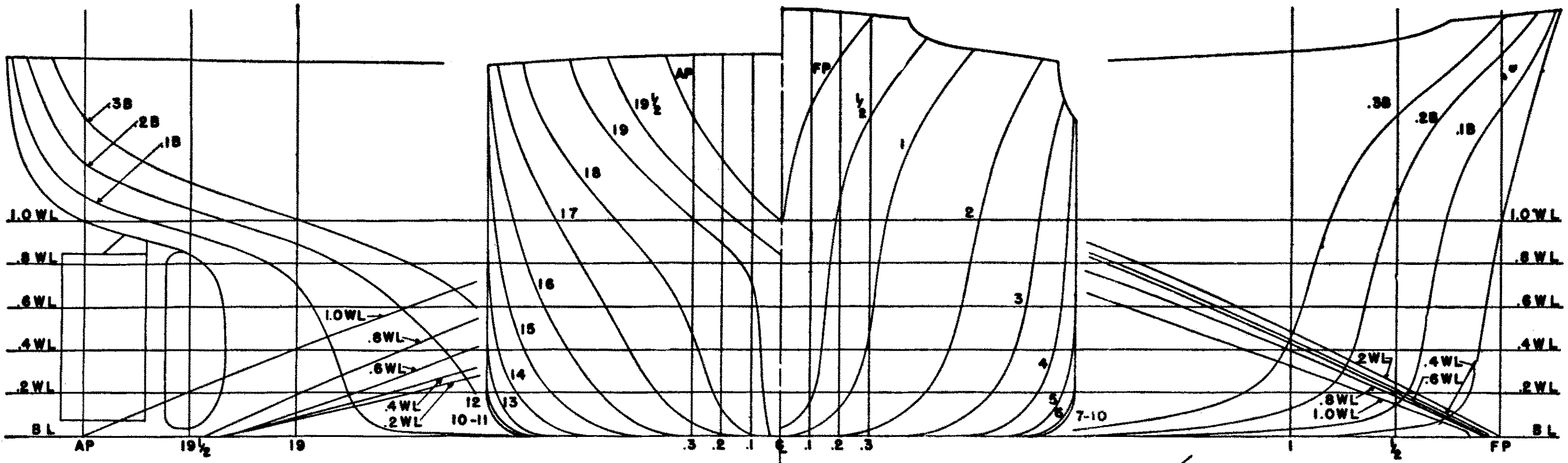

Lines

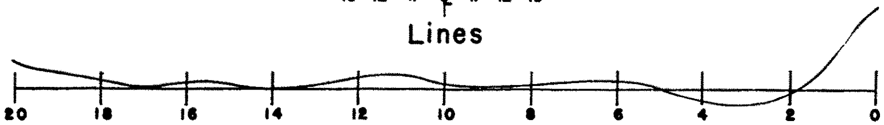

Wave Profile

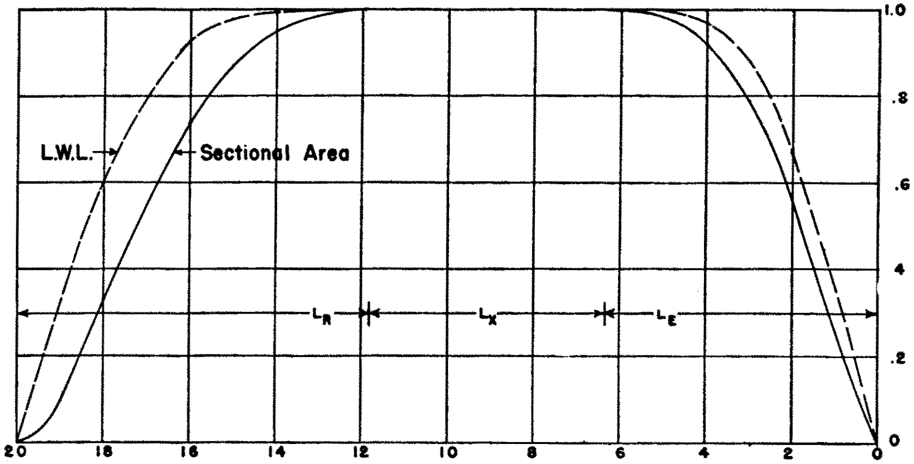

Sectional Area And Load Water Line

HULL DATA

L	600 Ft
B	83.51 Ft
H	30.64 Ft
$\Delta_{(SW)}$	32,800 Tons
∇	1,148,000 Ft^3
S	70,650 Ft^2
L/B	7.186
B/H	2.725
L_E/L	0.317
L_X/L	0.274
L_R/L	0.409
LCB/L	0.477
$L/\nabla^{1/3}$	5.73
$S/\nabla^{2/3}$	6.451
$1/2\,\alpha_E$	27.5°

C_B	0.746
C_P	0.752
C_X	0.993
C_W	0.821
C_{PE}	0.692
C_{PR}	0.633
C_{PF}	0.803
C_{PA}	0.701

PROPELLER DATA

D	21.85 Ft
P	17.82 Ft
P/D	0.815
MWR	0.216
PA/DA	0.398
BTF	0.051
No. Blades	4

Fig.1 LINES OF MODEL TANKER

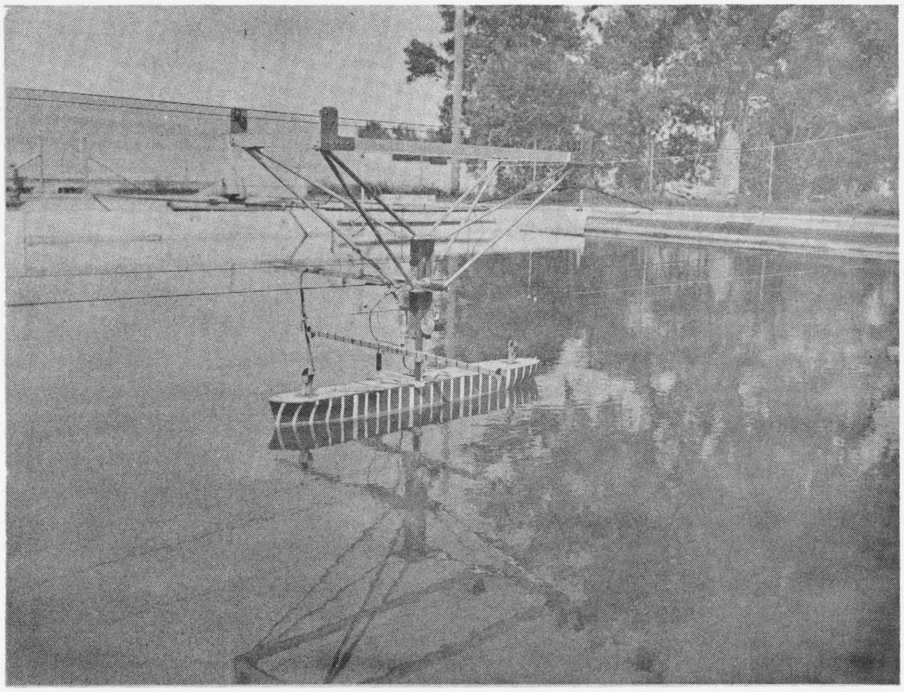

Fig.2 PHOTOGRAPH OF MODEL TANKER AND CARRIAGE

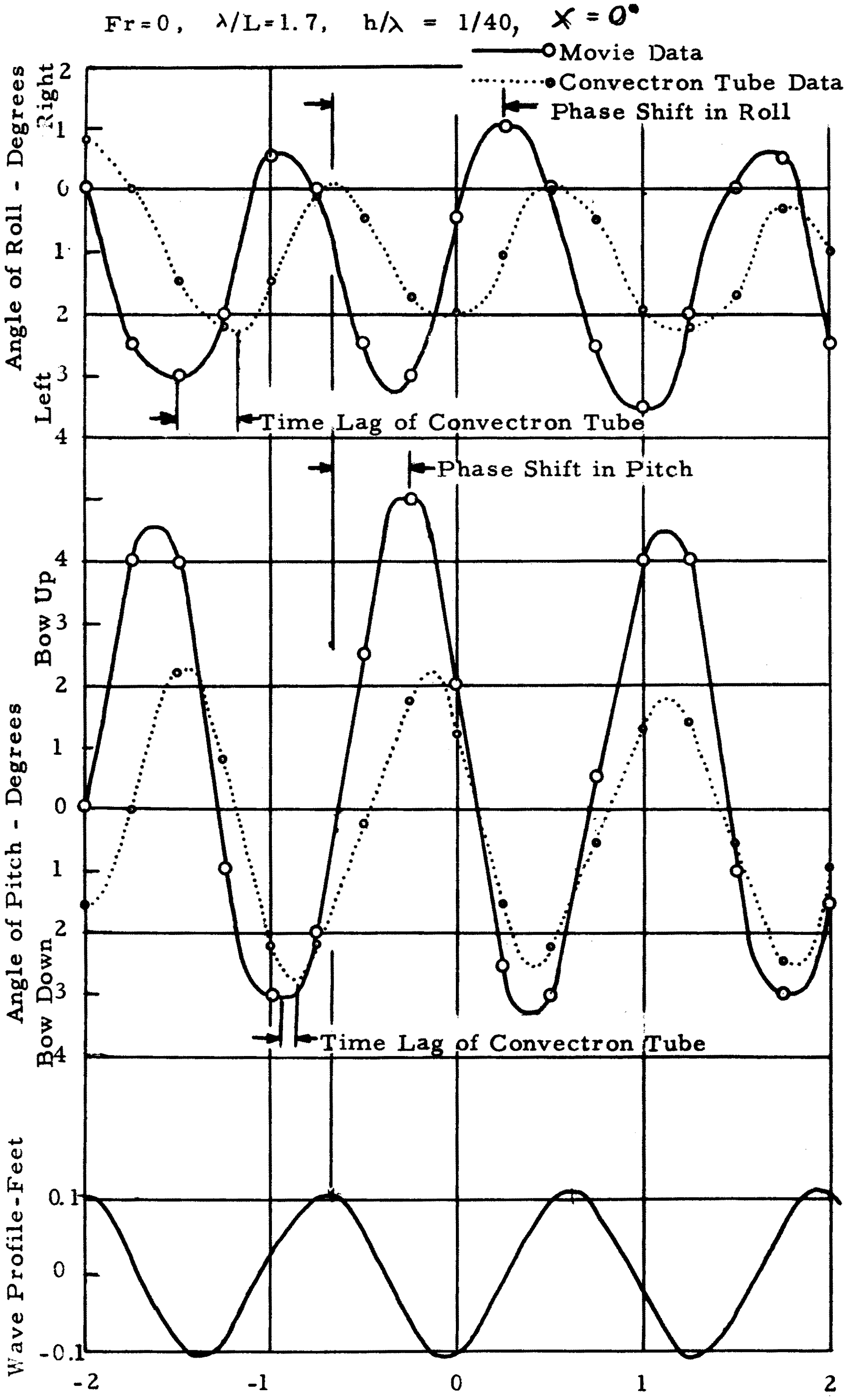

TIME HISTORY OF MOTION OF PITCH AND ROLL IN A REGULAR SEAWAY

Fig. 3

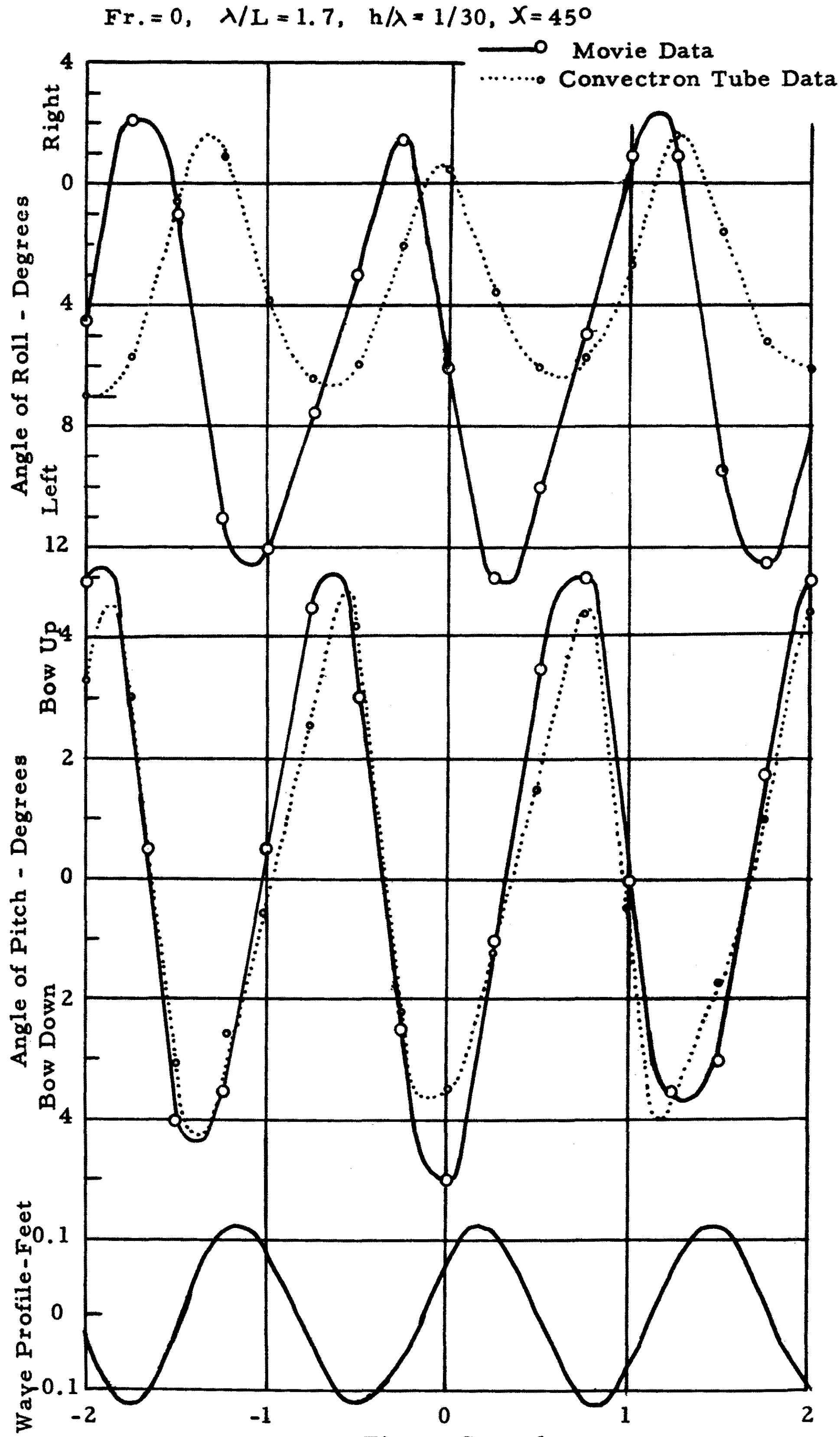

TIME HISTORY OF MOTION OF PITCH AND ROLL IN A REGULAR SEAWAY

Fig. 4

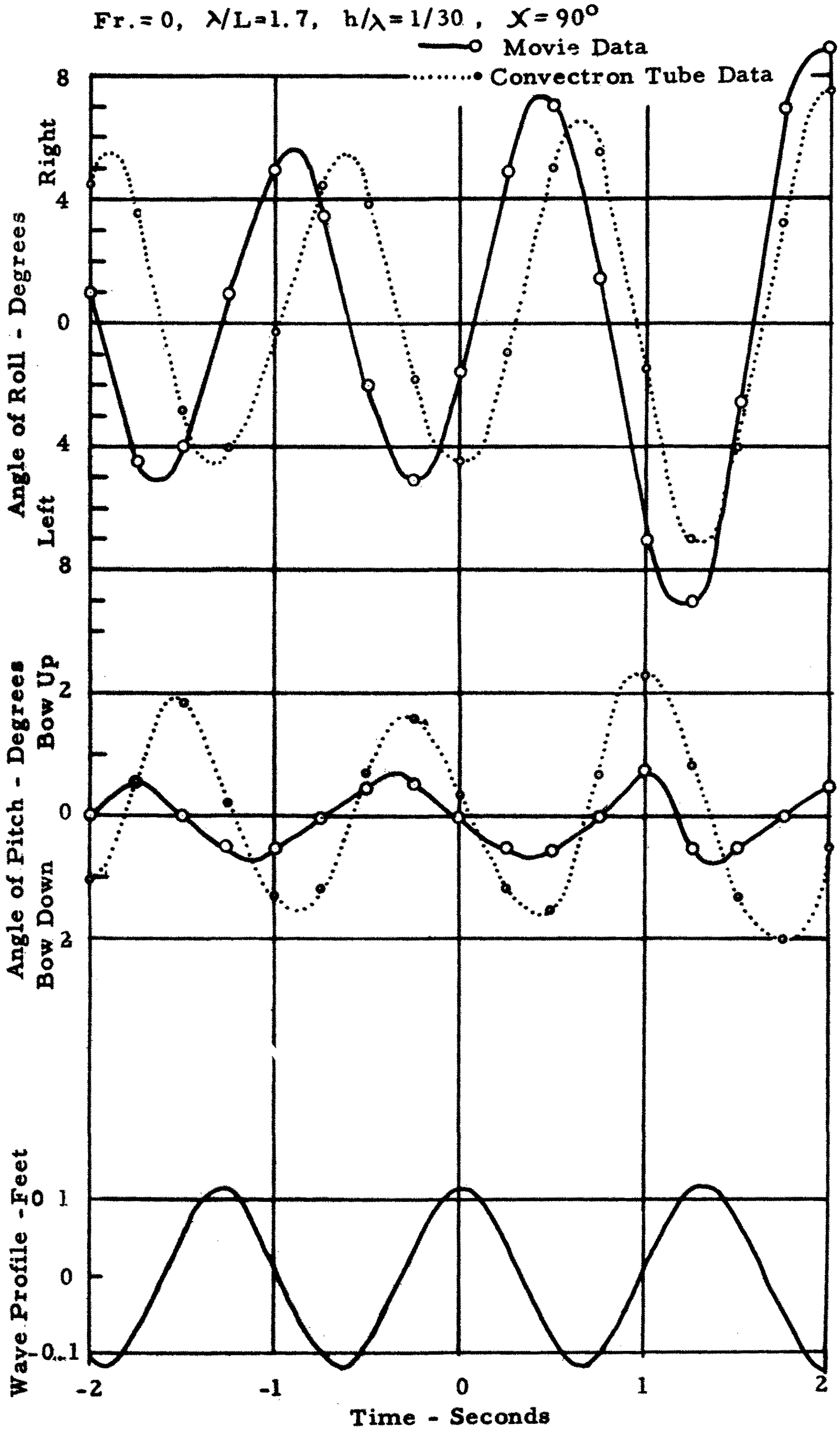

TIME HISTORY OF MOTION OF PITCH AND ROLL IN A REGULAR SEAWAY

Fig. 5

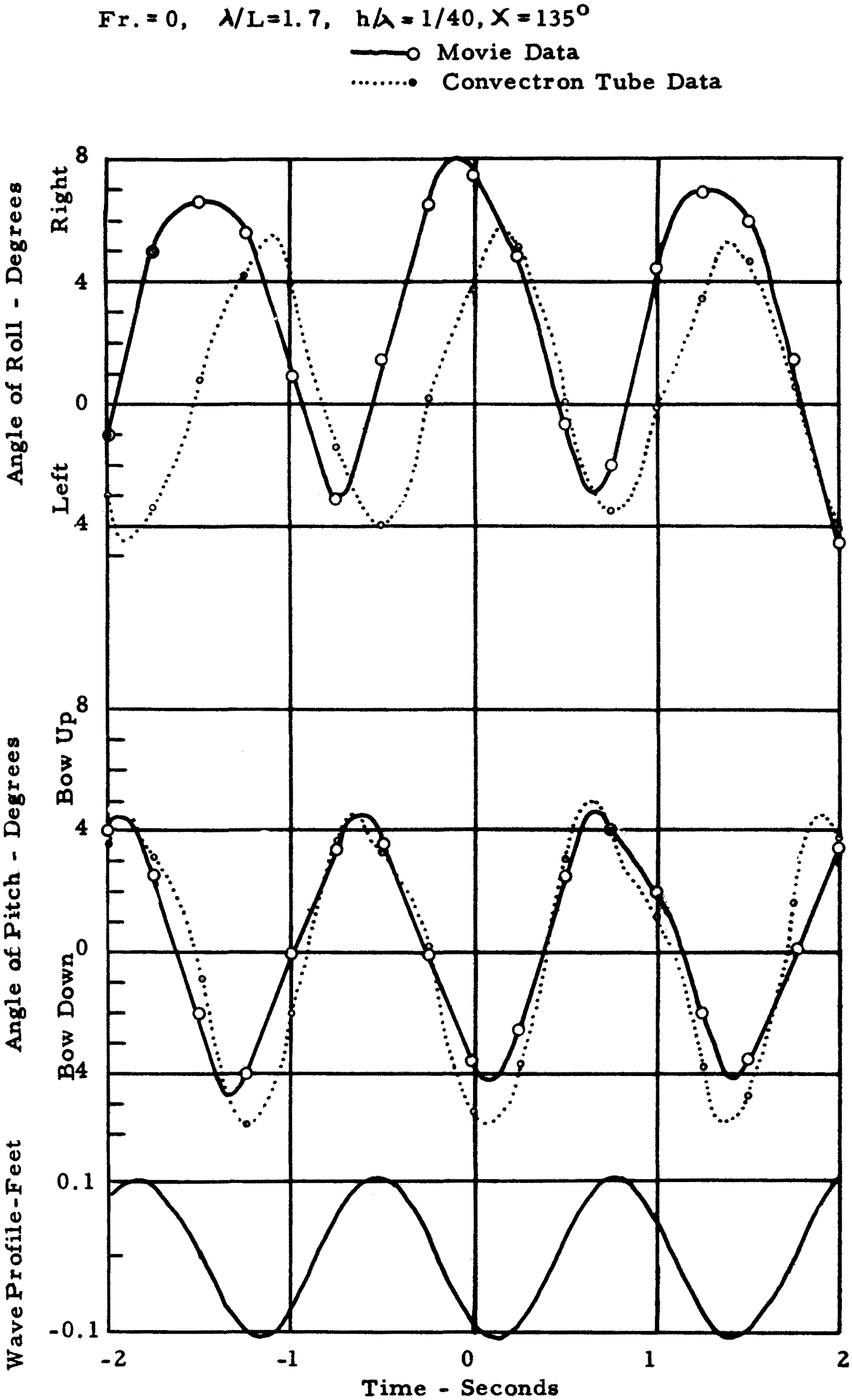

TIME HISTORY OF MOTION OF PITCH AND ROLL IN A REGULAR SEAWAY

Fig. 6

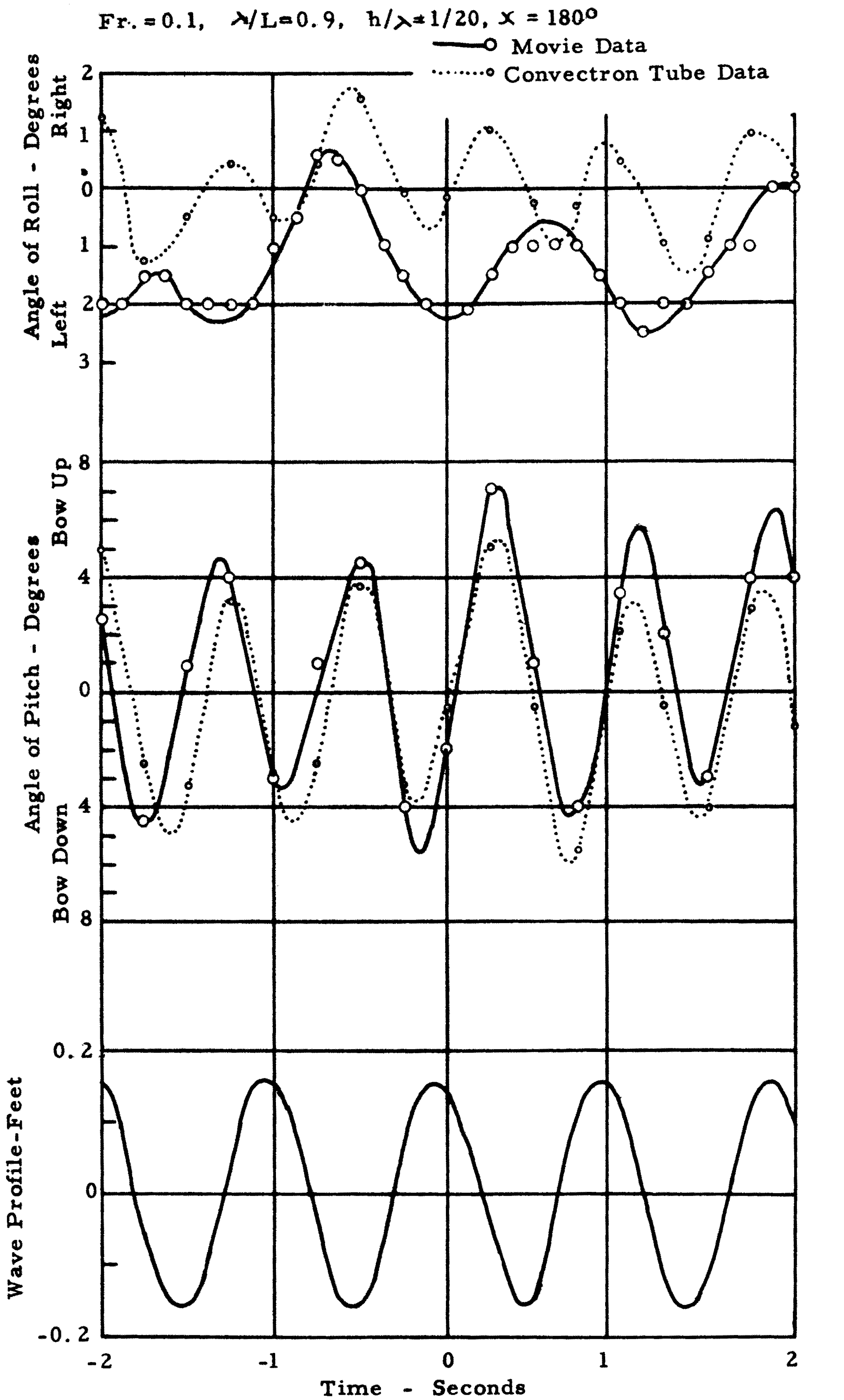

TIME HISTORY OF MOTION OF PITCH AND ROLL IN A REGULAR SEAWAY

Fig. 7

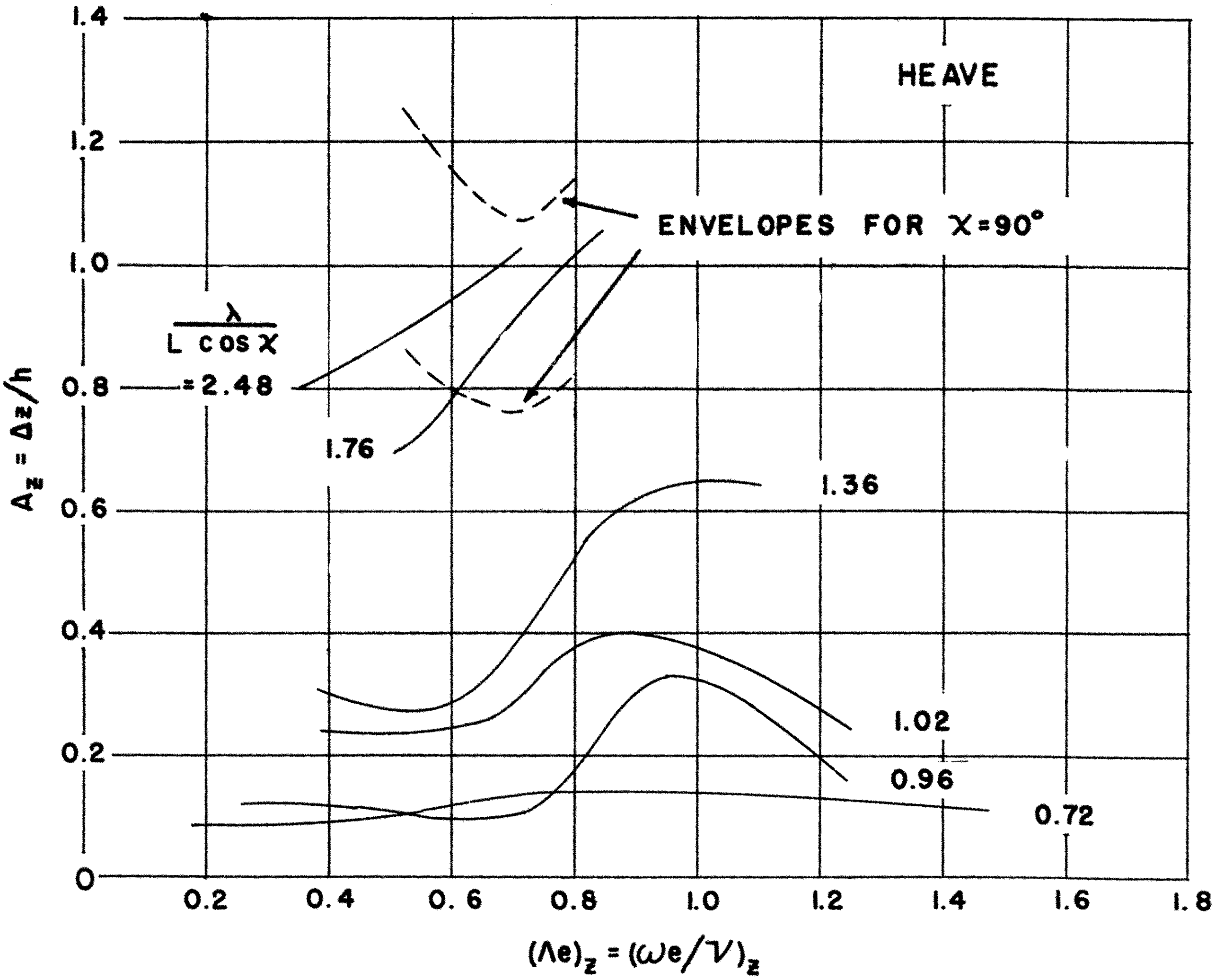

Fig. 8 HEAVE AMPLITUDE PARAMETER AS A FUNCTION OF TUNING RATIO

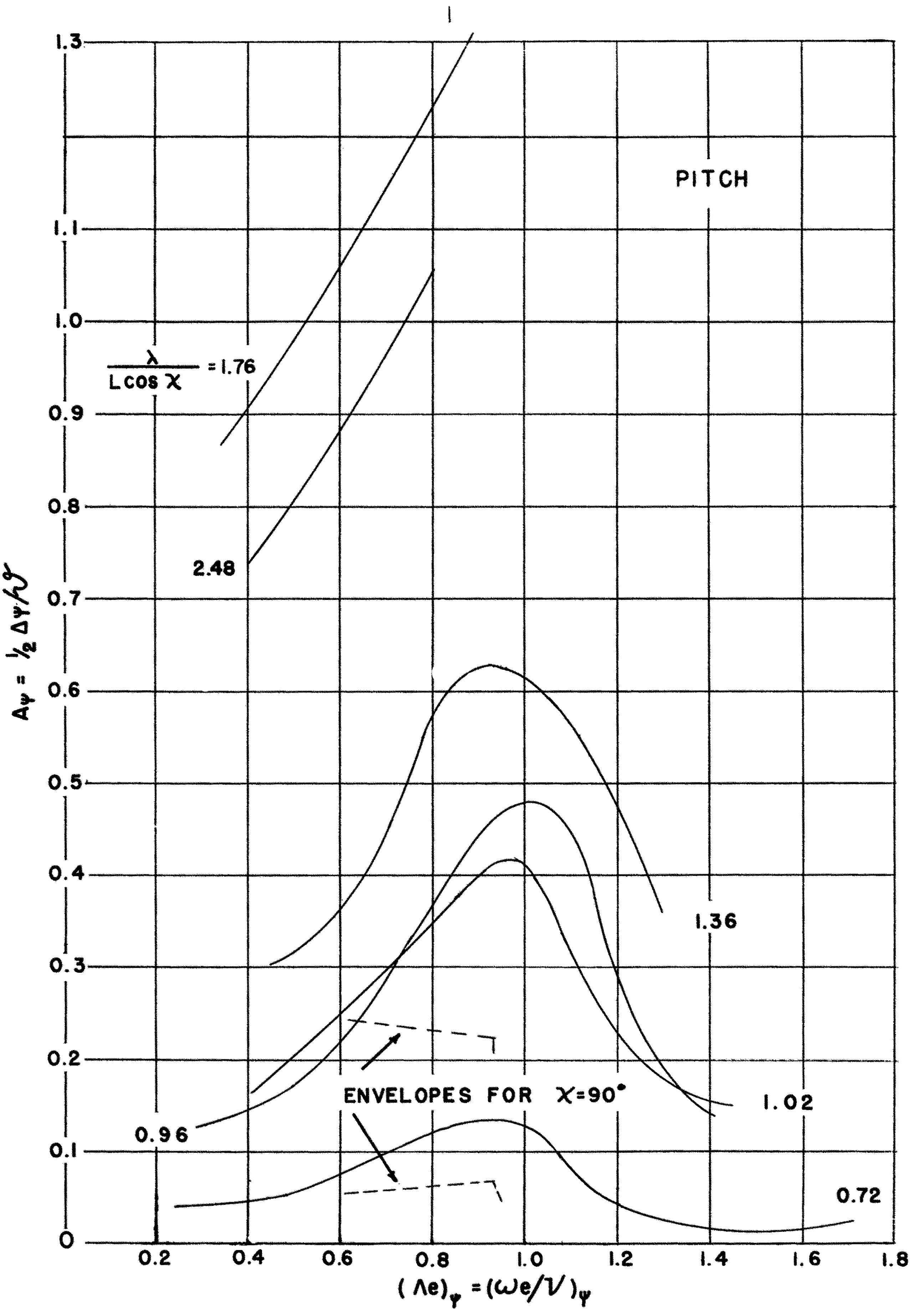

Fig. 9 PITCH AMPLITUDE PARAMETER AS A FUNCTION OF TUNING RATIO

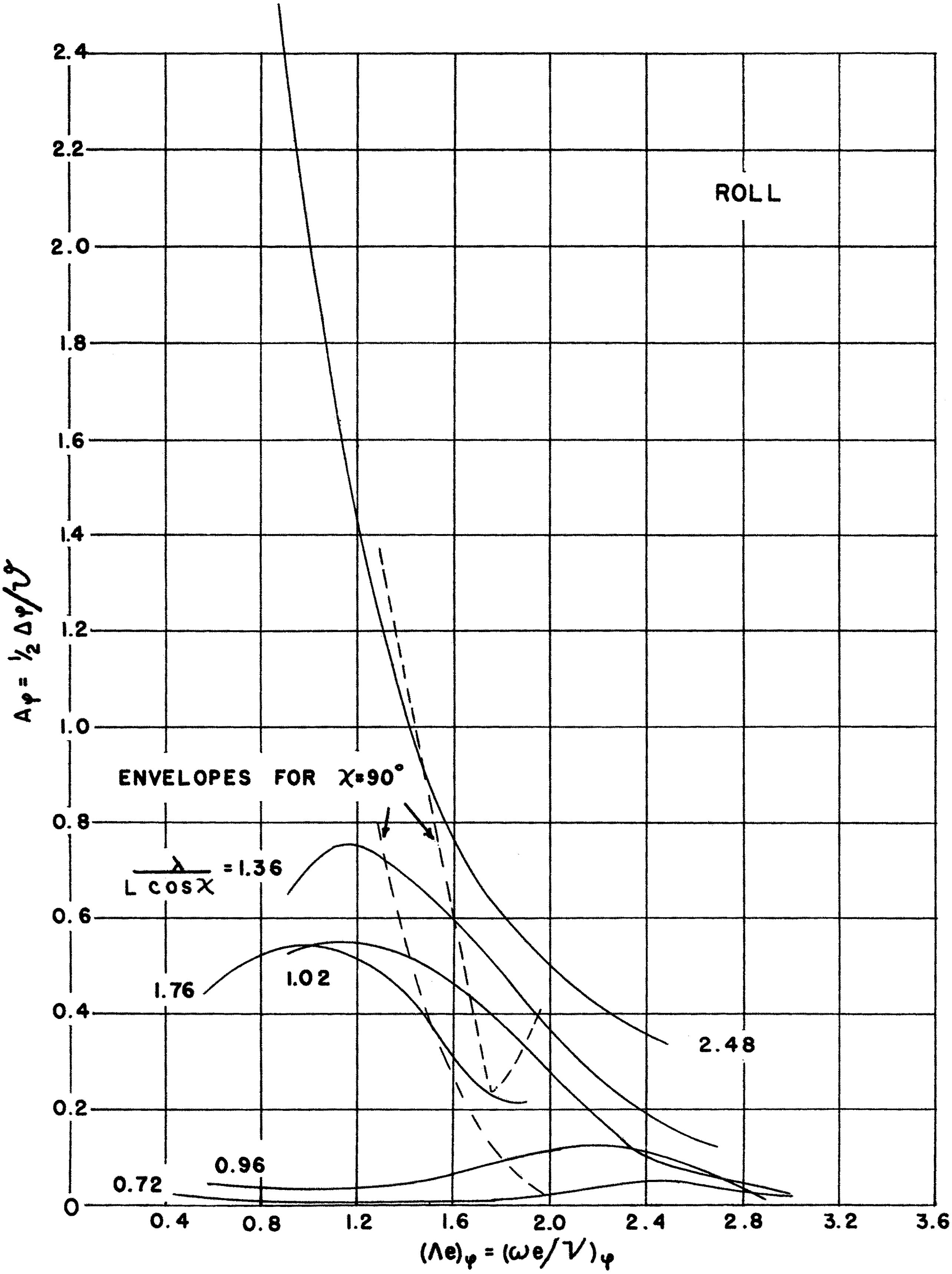

Fig. 10 ROLL AMPLITUDE PARAMETER AS A FUNCTION OF TUNING RATIO

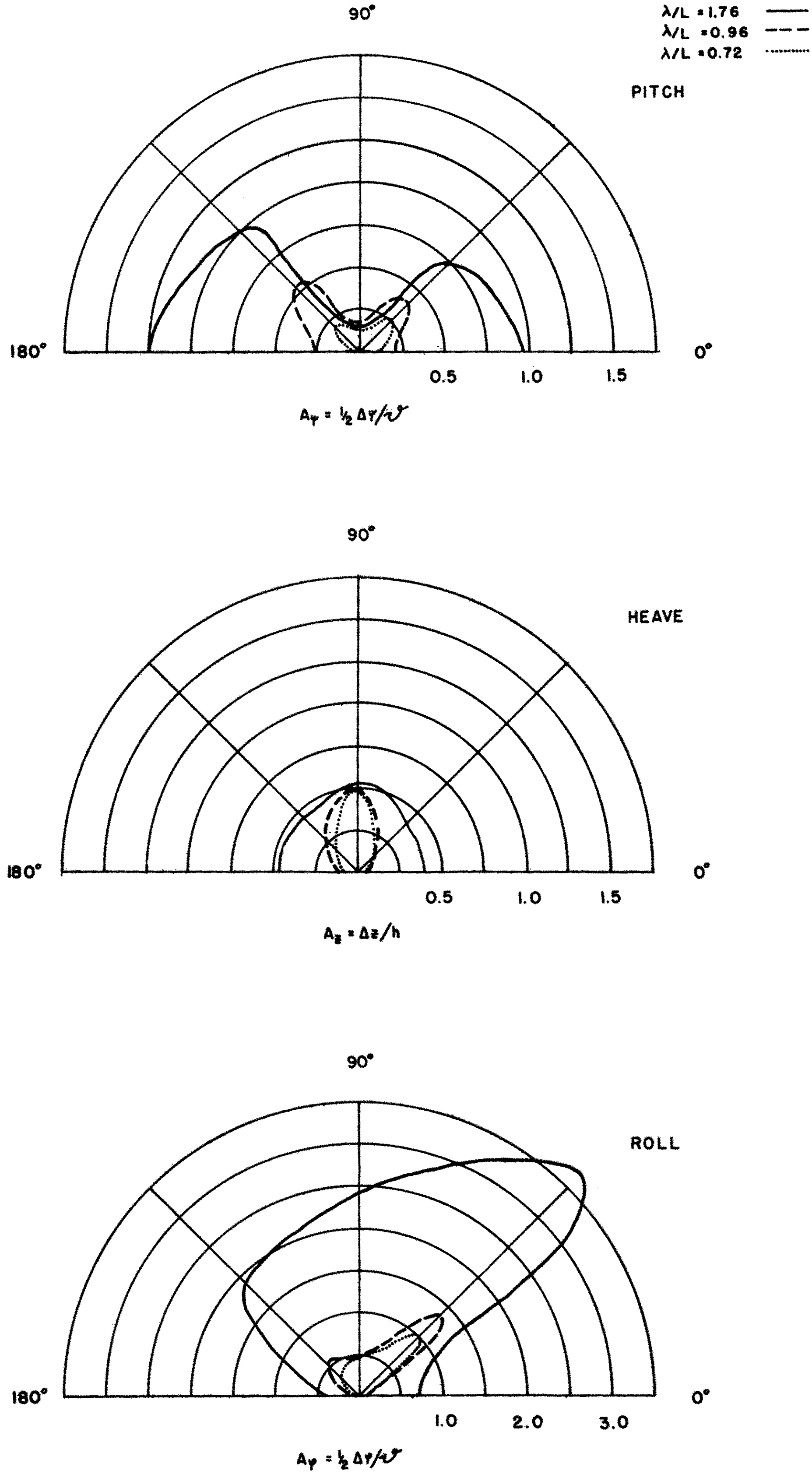

Fig. 11 AVERAGE AMPLITUDE PARAMETER AS A FUNCTION OF HEADING

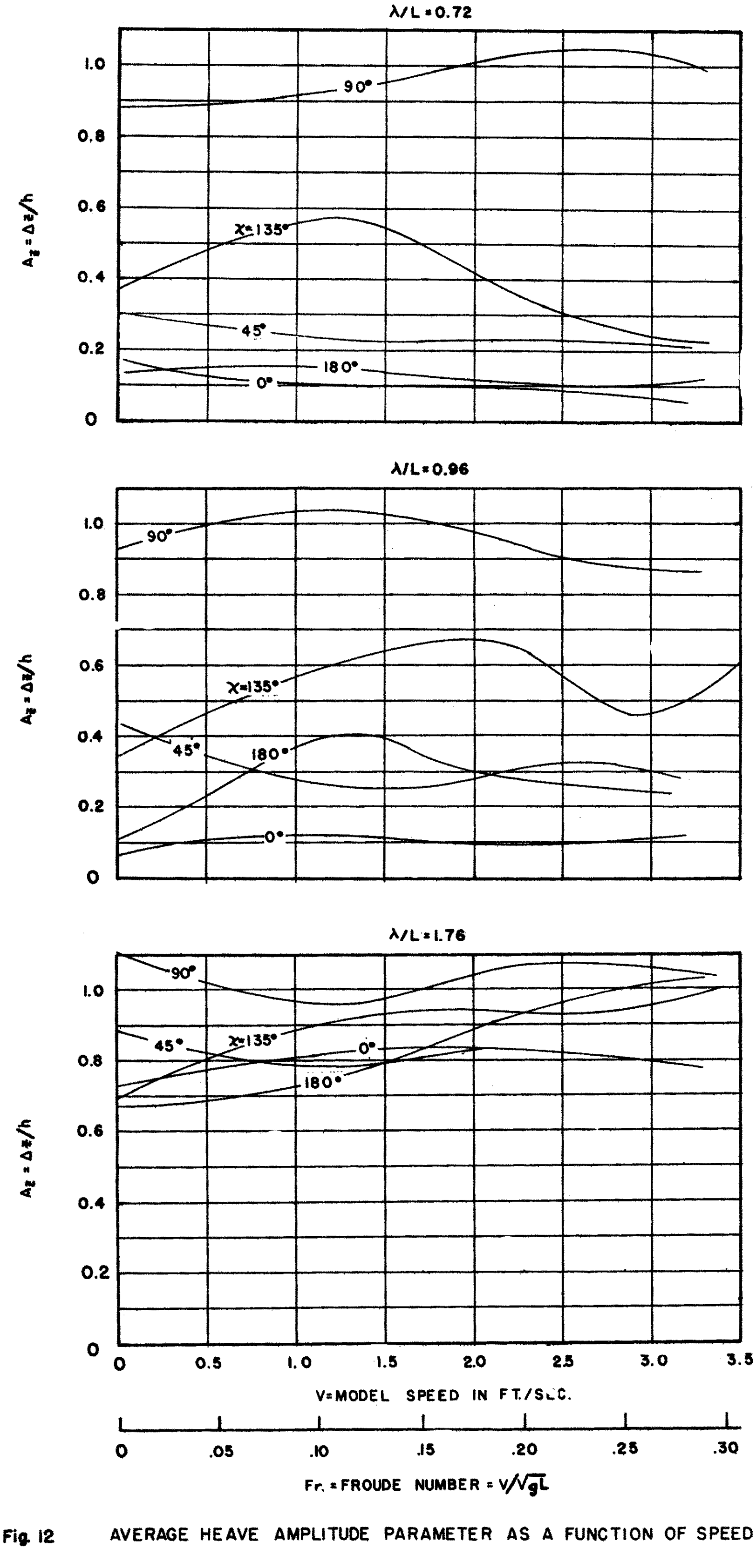

Fig. 12 AVERAGE HEAVE AMPLITUDE PARAMETER AS A FUNCTION OF SPEED

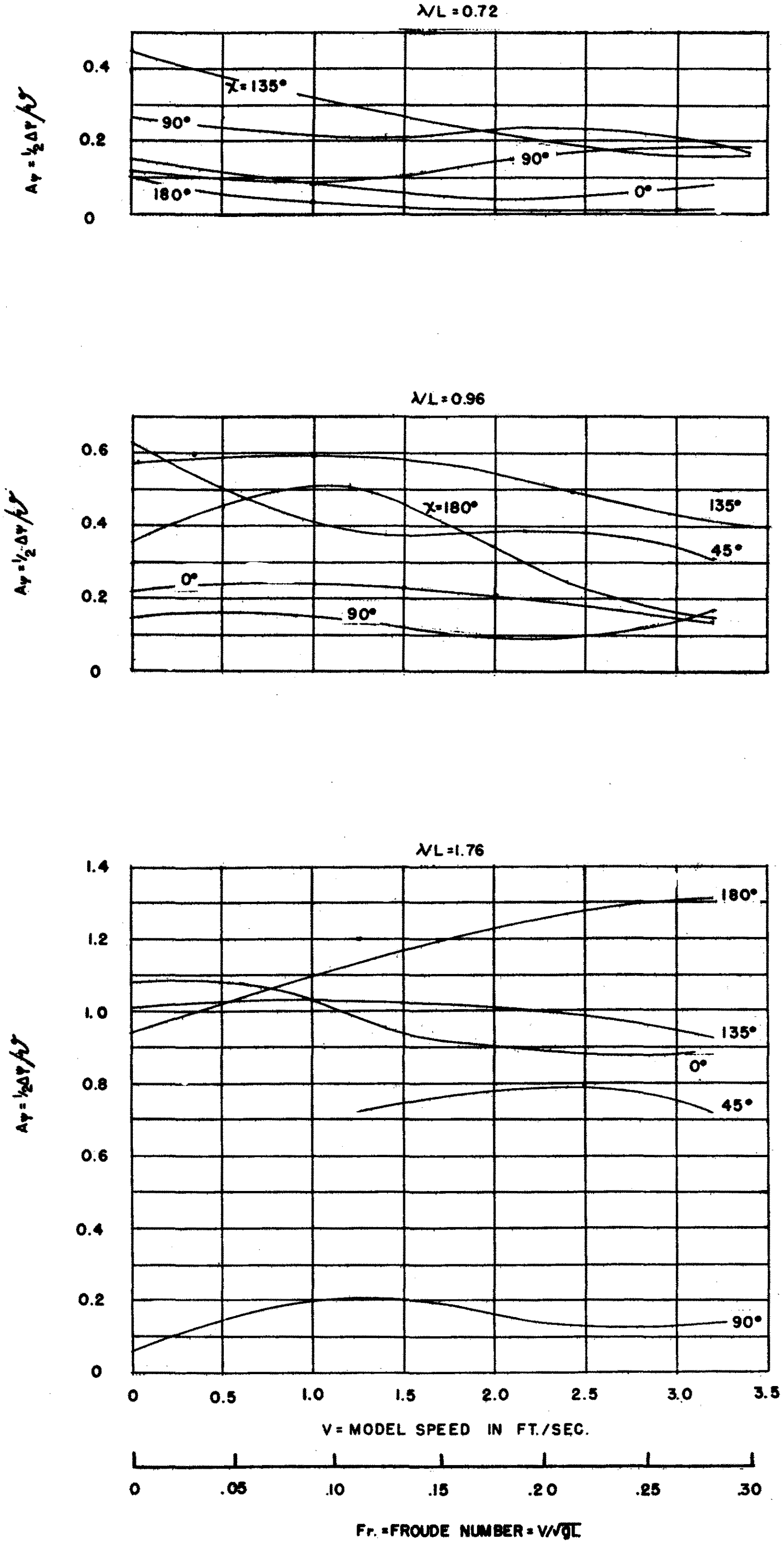

Fig. 13 AVERAGE PITCH AMPLITUDE PARAMETER AS A FUNCTION OF SPEED

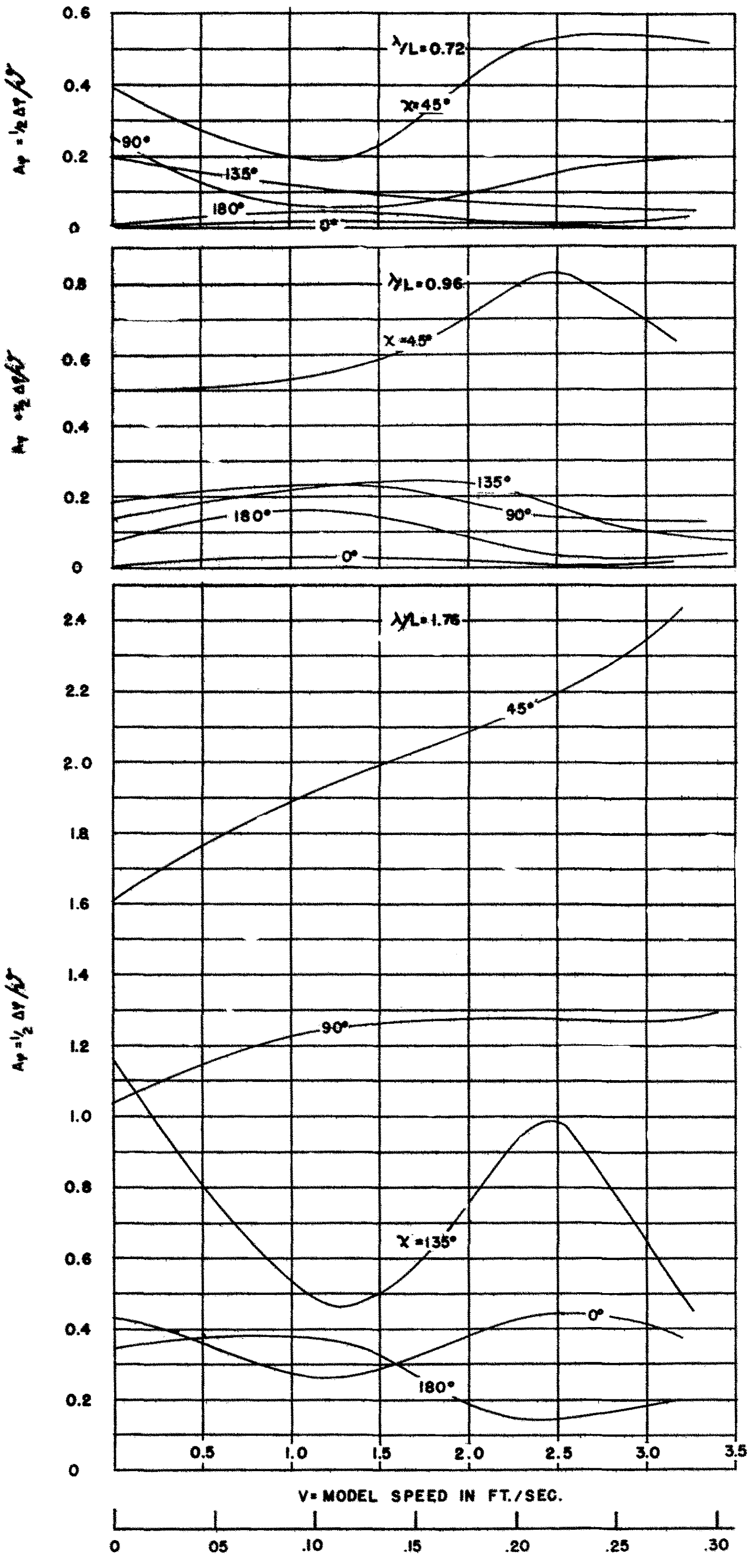

Fig. 14 AVERAGE ROLL AMPLITUDE PARAMETER AS A FUNCTION OF SPEED